

NPS ARCHIVE
1969
PENARANDA, F.

SHOCK TUBE INVESTIGATION OF THERMAL
CONDUCTIVITY IN NOBLE GASES

by

Federico A. Penaranda

United States Naval Postgraduate School



THESIS

SHOCK TUBE INVESTIGATION OF THERMAL
CONDUCTIVITY IN NOBLE GASES

by

Federico A. Penaranda

April 1969

T-151-42

This document has been approved for public
release and sale; its distribution is unlimited.

SHOCK TUBE INVESTIGATION OF THERMAL
CONDUCTIVITY IN NOBLE GASES

by

Federico A. Penaranda
Lieutenant Commander, Chilean Navy
Chilean Naval Academy, 1955
Chilean Naval Engineering School, 1961

Submitted in partial fulfillment of the
requirements for the degree of

MASTER OF SCIENCE IN AERONAUTICAL ENGINEERING

from the

NAVAL POSTGRADUATE SCHOOL
April 1969

NPS ARCHIVE

1969

PENARANDA, F.

~~402~~ P329 c.1

ABSTRACT

The Aeronautics Department shock tube has been developed and instrumented. The shock tube has been used in an experiment in which the thermal conductivity of argon has been determined in the temperature range of 1500 - 5000 °K and at relatively high pressures, 10 to 30 atmospheres.

TABLE OF CONTENTS

CHAPTER	PAGE
I. INTRODUCTION	11
II. DESCRIPTION OF EXPERIMENTAL EQUIPMENT	13
Shock tube	13
Instrumentation	23
Operating procedures	31
III. THEORY BEHIND SHOCK TUBE OPERATION	36
General theory	36
Theory for experiments	41
IV. EXPERIMENTAL RESULTS AND DISCUSSION	45
Description of experiment	45
Data reduction	46
V. CONCLUSIONS	52

LIST OF PLATES

PLATE		PAGE
1	SHOCK TUBE AT NAVAL POSTGRADUATE SCHOOL, MONTEREY, CALIFORNIA	14
2	VIEW OF DRIVER END	19
3	DRIVEN END VACUUM SYSTEM	22
4	TRACE OF TEMPERATURE SENSITIVE RESISTANCE DETECTORS	34
5	TRACE OF HEAT TRANSFER THIN FILM GAUGES	35
6	TABULAR SOLUTION OF EXPERIMENT	47

LIST OF FIGURES

FIGURE		PAGE
1	Schematic of shock tube sections	15
2	Schematic of driver end section	18
3	Schematic of driven end vacuum and filled system	20
4	Thin film gauge arrangement	26
5	Temperature coefficient of resistivity (α) for heat transfer thin film gauge	28
6	Schematic of electronic arrangement	29
7	Schematic for thin film gauges	30
8	Thermodynamic history of the shock tube	37
9	Plot of distance vs. time in shock tube after diaphragm is broken	39
10	Plot of exponent "a" vs. residual	49
11	Dimensionless plot of data and best curve fit	51

TABLE OF SYMBOLS

a	sound speed
C_p	heat capacity per unit mass at constant pressure
E	voltage
I	electric current
k	heat conduction coefficient
M	Mach number
P	pressure
q	rate of heat transfer
R	electrical resistance
R	gas constant
S	entropy
t	time
T	absolute temperature
u	velocity along x-axis
V	volume
X	distance
α	temperature coefficient of resistivity
β_s	calibration factor
γ	specific heat ratio C_p/C_v
η	similarity parameter
ψ	stream function
ρ	mass density

CHAPTER I

INTRODUCTION

Although the shock tube has been known as an experimental device in the study of gas dynamics for the past 70 years^[1] since Paul Vieilli in France (1899) made first known use of it, it was not until the early 1940's when better methods and equipment were developed to measure the phenomena occurring in the gases tested, that it began to enjoy much application or widespread use.

With the rapid technological development of electronic measuring equipment permitting the use of fast response high sensitive instruments the shock tube has become a very useful experimental tool for study and research in the fields of gas dynamics. Specific applications include the study of shock waves, shock fronts and interactions, aerodynamics for the study of the subsonic, transonic and supersonic flow regions, as well as a means of driving hypersonic wind tunnels^[1], chemistry for the study of high temperature gas reactions^[2], physics for study of conversion of energy from one form to another, i.e., translational to energy of internal vibration or rotation of molecules^[2], in the field of planetary-entry fluid physics connected with the design of the spacecraft's heat shield^[7] and many other applications.

The purpose of the work presented in this thesis, was first to install instrumentation and leave in working condition a newly developed shock tube for the Department of Aeronautics of the Naval Postgraduate School and after that was accomplished, use it to determine the thermal conductivity of a noble gas (argon in this

case) in the range from 1500 to 5000 degrees Kelvin at relatively high pressures i.e. 10 to 50 atmospheres. Although several authors have reported results in this type of experiment^{[6],[10]}, they all have been done at low pressure i.e. around 1 atmosphere and data for the same experiment worked here was not available. The value obtained here, for the calibration parameter of the shock tube, β_s , is some 15% higher than similar parametric values verified in previous shock tube experiments^{[6],[10]}, but the initial conditions to determine it, where again different, in this case, the calibration runs were accomplished in the range from 1 to 10 atmospheres of pressure.

As a preview of the following work, Chapter II describes the equipment, instrumentation and procedures used in the course of this work. Chapter III is related to the general theory behind shock tube operation as well to the theory related to the experiment accomplished. Chapter IV is devoted to the experiment itself, the data reduction and presentation of results, and Chapter V gives the conclusions of the present work.

It is proper to hereby acknowledge the kind assistance of several people who contributed to the completion of this work. The author wishes to express his appreciation to his advisor, Dr. Daniel J. Collins, for his guidance and assistance during the entire time this work was carried out; to Mr. Dana Maberry and Mr. Norman Leckenby for their cooperation and assistance in the performance of the experimental program; to Mr. Robert Besel for his assistance with the graphics work.

Last, but not least, the author is particularly indebted to his wife, Maria Angelica, for her assistance in the preparation of the manuscript and for her understanding and patience during the entire course of studies.

CHAPTER II

DESCRIPTION OF EXPERIMENTAL EQUIPMENT

I. SHOCK TUBE

General

The shock tube shown in Plate I was constructed at the Naval Postgraduate School, Monterey, California. The equipment has been installed in one of the Aeronautical Laboratories of the School.

Shock tube configuration was chosen with two definite purposes in mind, namely to be used as a laboratory equipment for the courses in the Gas Dynamics option in the Aeronautical Engineering curricula at the School and at the same time as a research aid in the field of high temperature gas dynamics.

Essentially a shock tube consists of a rigid cylinder (although different cross-sectional shapes are possible), divided into two sections by a thin diaphragm mounted normal to the axis of the tube. The principle of operation calls for a pressure difference to exist across the diaphragm. The high-pressure side is called the Driver section and a low pressure region is called the Driven section.

Figure I shows a schematic of the shock tube sections concerned. The material used is a stainless steel tube, 3 in. in internal diameter, with a wall thickness of 0.5 inc. and a highly polished internal surface. The overall length of the tube is approximately 25 ft. constructed in four sections of different lengths. This arrangement facilitated the construction of the tube and at the same

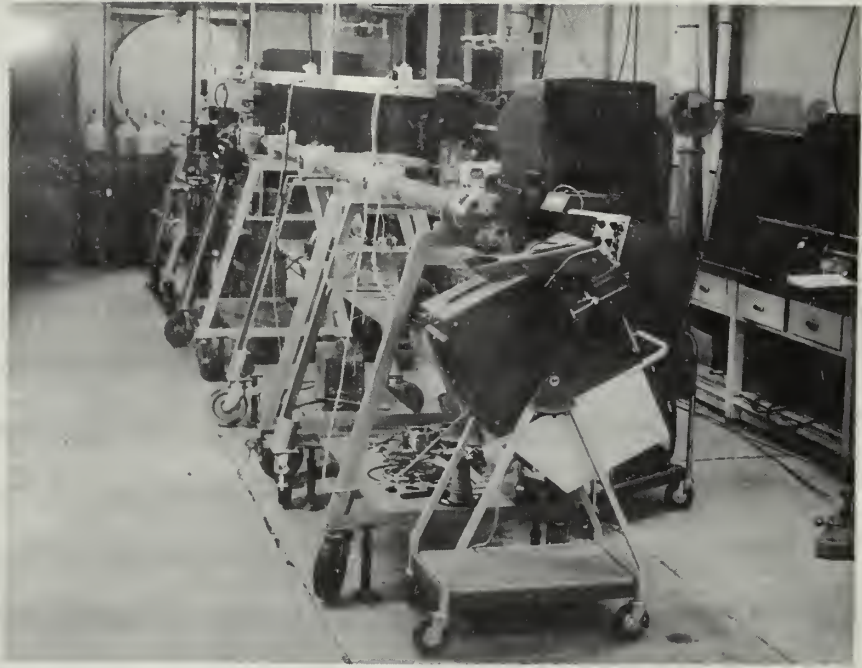


PLATE I

SHOCK TUBE AT NAVAL POSTGRADUATE SCHOOL
MONTEREY, CALIFORNIA

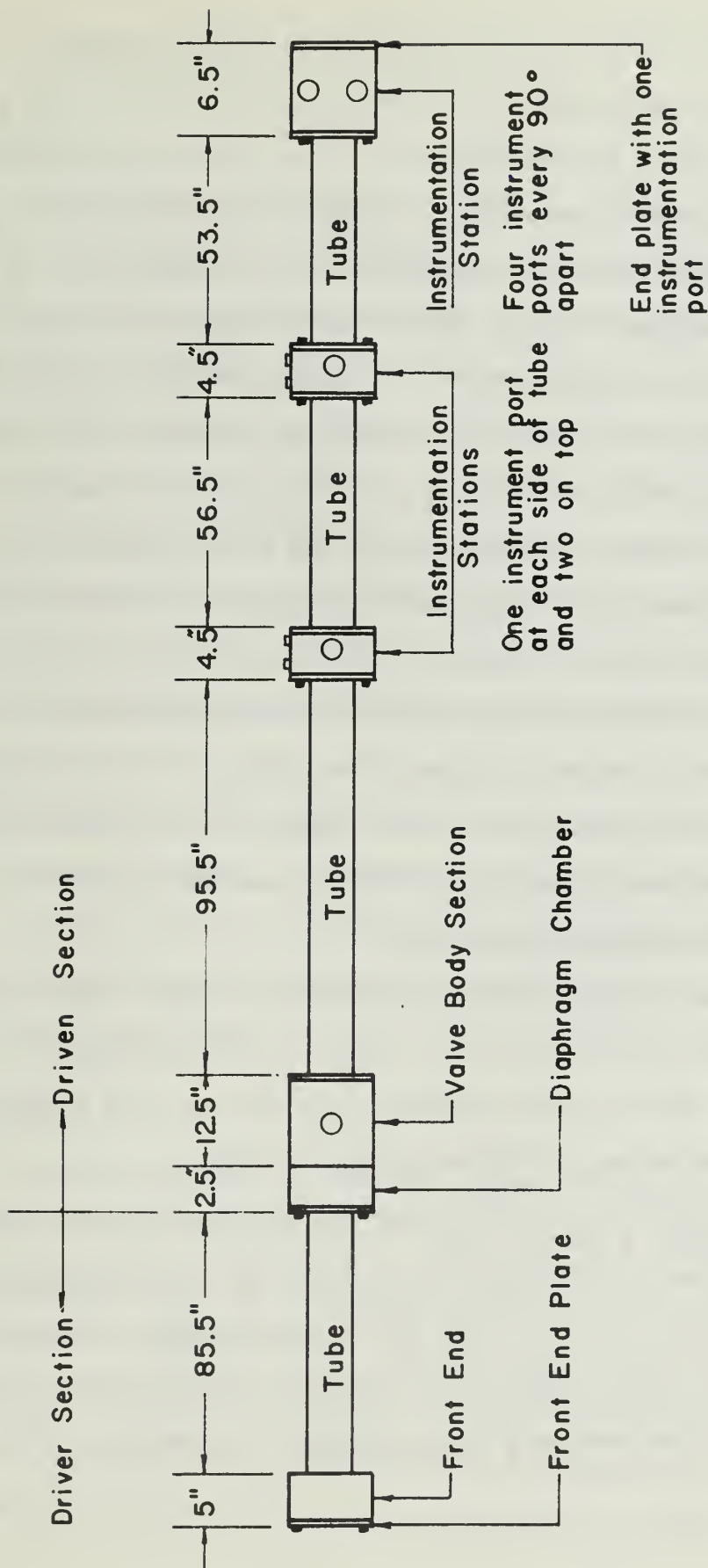


FIGURE 1
SCHEMATIC OF SHOCK TUBE SECTIONS

time provides flexibility in the case that different driver or driven tube lengths are required. The first section of tubing, with a length of 7 ft. 3 in. is the driver section. The other three pieces of the tube make up the driven section. Between the driver section and the driven section is inserted a transition section which holds the valve body and diaphragm section. Connecting the three tube sections that make up the driven end are two 6 in. outside diameter instrumentation sections of 4.5 in. length. These have two instrumentation ports at each side of the tube and two on the upper part, intended to house the different types of detectors which can be used, such as pressure-transducer, shock detectors, temperature-sensitive resistance (thin metal film), ionization detectors, light screen schlieren, etc.

The end of the shock tube has another instrumentation station, with four ports located 90° apart of each other. The end plate of the tube, also has provision for the insertion of instrumentation. All instruments and plugs used in the instrumentation sections are flush mounted with the inside wall.

Different sections are bolted together and end flanges and joints, are sealed by means of Viton "O" rings. The ratio between the length of the tube and the inside diameter is 76 and the ratio between the length of the driver and driven section is 0.368.

As indicated before, the driver and driven section are separated by a diaphragm. In this shock tube, there are two diaphragms separated by a distance of 2.5 in. called the diaphragm chamber, which will be described later, permits a very ingenious but simple way of obtaining a rather precisely controlled bursting pressure. The shock

tube assembly is supported as shown in Plate I.

Driver End

A very important consideration in the operation of the shock tube is the vacuum and gas filling system required. Figure 2 shows a schematic of the system used for the driver end section of this tube. The vacuum pump evacuates the high pressure region of any remaining gas, air and moisture before the section is filled with the gas to be used. Gas is admitted to the front end section of the shock tube from a high pressure bottle of gas by means of tubing through a regulator valve connected directly to the bottle and a pressure control valve located beside the tube. By means of a "T" connection two high pressure bottles of either the same or different gases, can be used in the charging of the shock tube. The pressure of the gas in the tube is obtained from a pressure gauge located in the upper part of the front end section of the tube. To provide a means of evacuating the gas, after the shock tube has been fired, a bleed valve is located in the bottom part of the front end section. Plate 2 shows the actual set-up of the driver end section.

Driven End

The vacuum system of low pressure region or driven end is an important part of shock tube operation. Figure 3 shows a schematic drawing of the different parts which make up the vacuum system. Its details and purposes are described below. Basically the main concern faced in the design of the vacuum system, is the range of vacuum required. With this criteria in mind, the selection of a system which will be adequate and expeditious, is of prime importance for optimum utilization

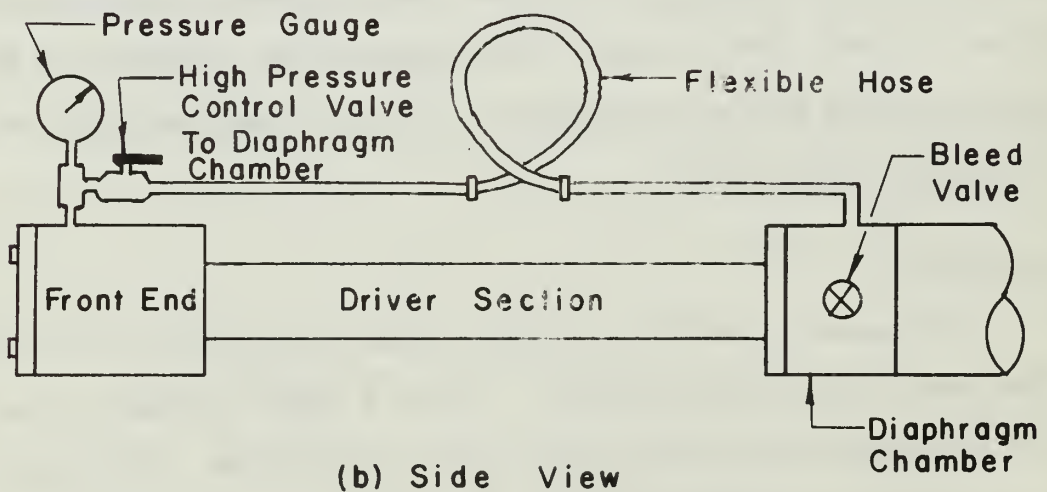
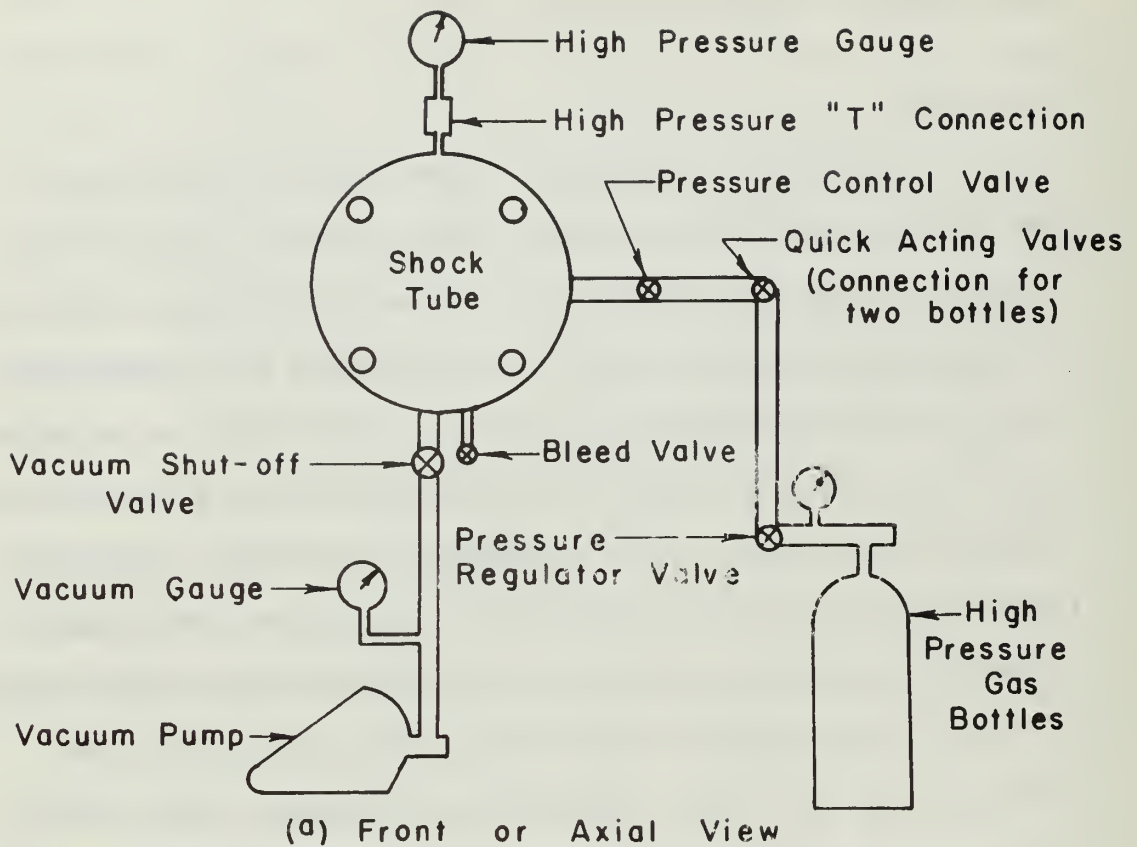


FIGURE 2

SCHEMATIC OF DRIVER END SECTION

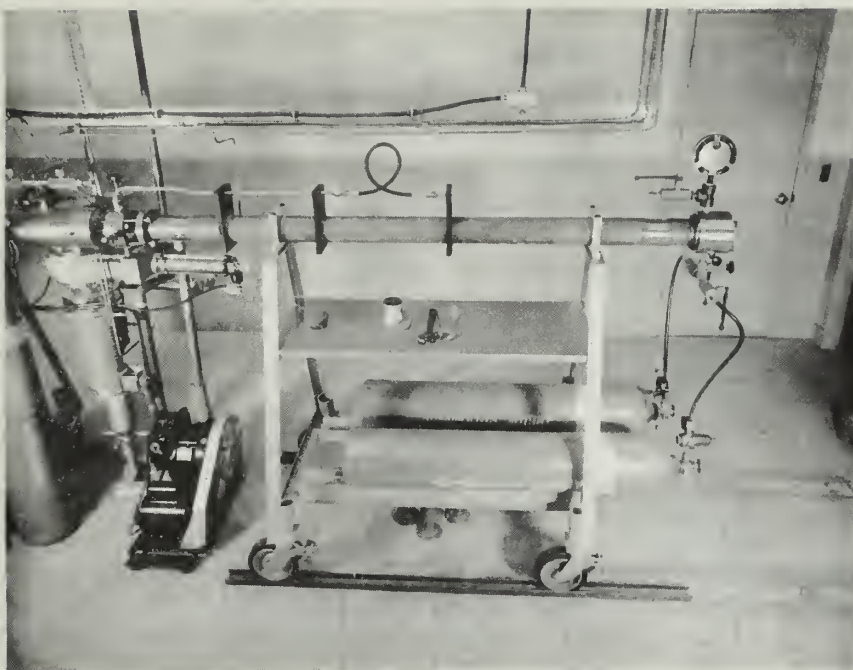


PLATE 2
VIEW OF DRIVER END

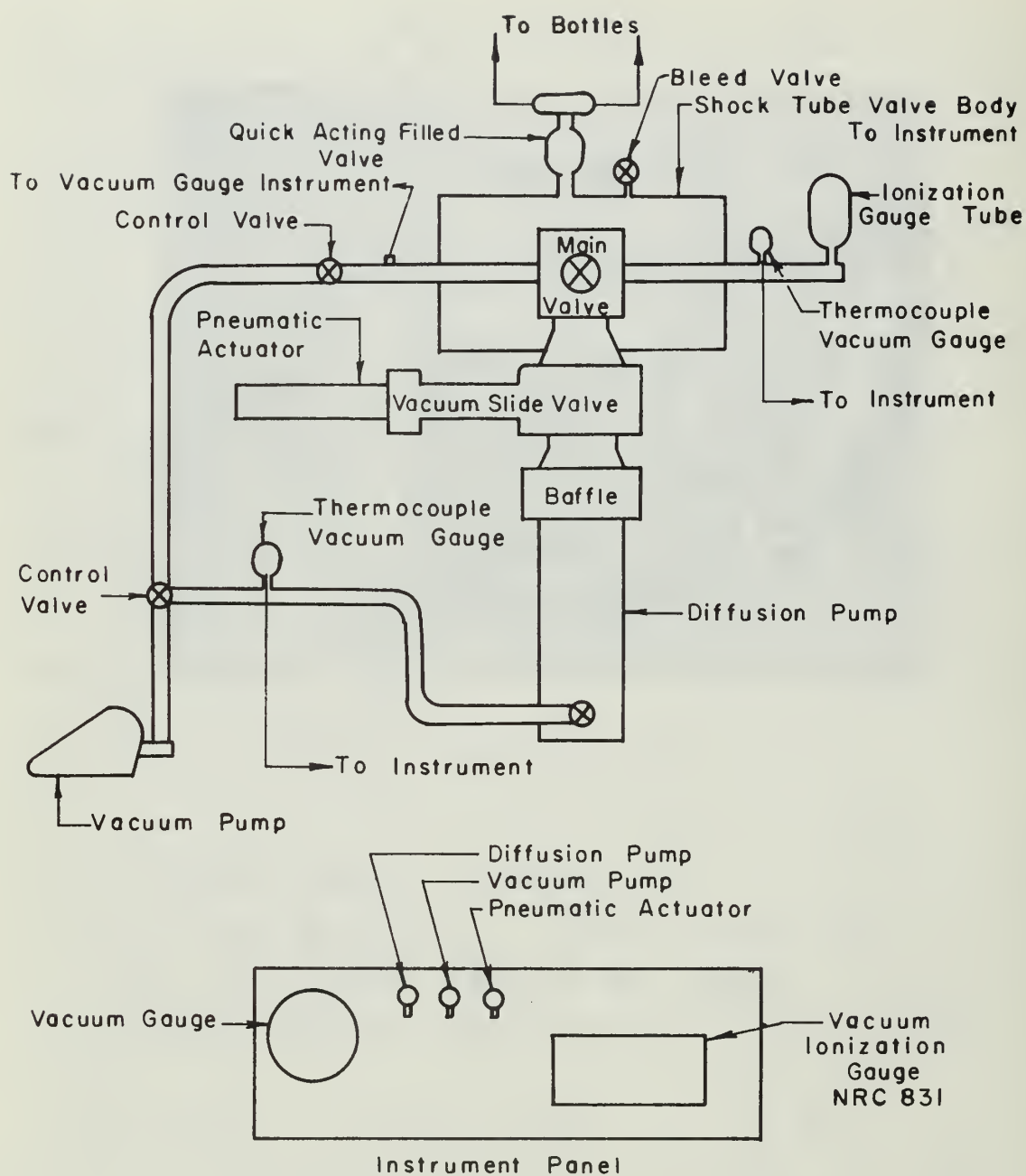


FIGURE 3

SCHEMATIC OF DRIVEN END VACUUM AND FILLED SYSTEM

of the shock tube.

Connected directly to the shock tube valve body is the main valve, which controls the operation of the vacuum system. The main valve is connected to a General Electric, Model 5KC45PG4X, vacuum pump which is designed to initially evacuate the driven end and is capable of pulling up a vacuum of approximately 10^{-3} mm. of mercury. Also connected to the main valve is a diffusion pump, which is capable of pulling up vacuums of 10^{-11} torr. The diffusion pump used, is manufactured by National Research Corporation (NRC), a subsidiary of Norton Company of Newton, Massachusetts. The system also consists of a Circular Chevron Cryo-Baffle and a pneumatically operated High Vacuum Slide Valve, both manufactured by NRC. The equipment is shown schematically in figure 3. Two thermocouple vacuum gauges and one ionization gauge tube, are used to measure the pressure. The thermocouples gauges are manufactured by NRC and the type used is 0531. The vacuum ionization control gauge instrument is also manufactured by NRC and its model is NRC 831. The ionization gauge tube is a RG 75-K manufactured by Vacuum Electronics Corporation (Veeco), Long Island, New York. The vacuum gauge instrument, vacuum ionization gauge instrument and the control switches for the diffusion pump, vacuum pump and pneumatic actuator for the high vacuum slide valve are mounted in an instrument panel for easier control and operation of the vacuum system. Plate 3 shows the actual set-up of the driven end vacuum system and instrument panel respectively.

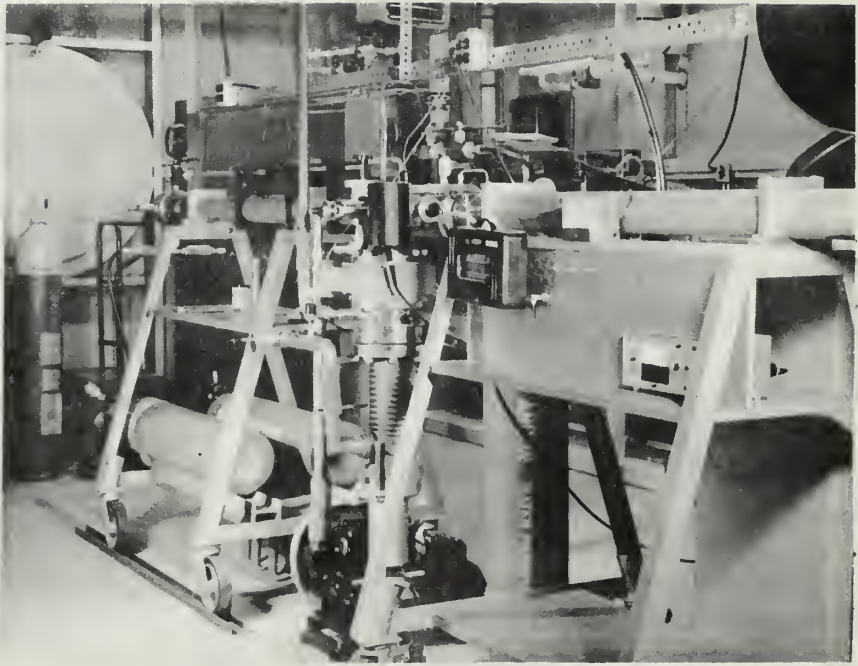


PLATE 3
DRIVEN END VACUUM SYSTEM

II. INSTRUMENTATION

General

The successful use of the shock tube depends entirely on suitable instrumentation for the required flow measurements. Although the type of instruments to be used depend largely on the experiment being run, accuracy needed, and money available, they all require a precise and fast response, since the duration of the shock wave in the tube is of the order of milliseconds. Consideration is given here to the actual instrumentation used in the shock tube at the Naval Postgraduate School.

Temperature sensitive resistance detectors

One of the fundamental measurements in shock tube tests is that of the shock speed. One way to accomplish this measurement is by using temperature sensitive resistance detectors or most commonly known as thin film gauges. These devices are of local manufacture, using a short length of glass or pyrex about 0.25 in. in diameter, with one flat end and edges carefully polished. A film of Liquid Bright Platinum No. 05, manufactured by Engelhard Inc., East Newark, New Jersey was used and a thin strip was painted over the flat end and extended through the sides of the tube; the film should be around 1/32" in width and its length and thickness such that the resistance is about 100 ohms; after that is accomplished it is let to air dry for a minimum of one hour, then baked in an oven to 1240°F for 20 minutes and then air cooled; the process is completed by annealing three times to 1100°F for 1 hour, allowing complete air cooling every time. Leads are

soldered to the sides of the gauge by using Eccobond Solder V-91, a product of Emerson & Cuming Inc., Canton, Mass., and after that, the gauge is placed on a phenolic plug, for insulation purposes, to hold it in place in the instrumentation port plug of the tube, as shown in Figure 4. Although "O" rings are provided for sealing, in order to avoid any possibility of leak through the thin film and the phenolic plug, the free space between them was filled up with Epoxy made with APCO 210 resin and APXO 180 hardener, products of Applied Plastic Co., Inc. (APCO), El Segundo, California.

The response of a thin film gauge operates, dependent on a change in resistance with a change in temperature of the thin metal film. In the case of the shock tube, this rise in temperature is provided by the shock wave. With a constant current passed through the metal film, a rapid increase in voltage is obtained as the shock wave passes over the gauge. This voltage properly amplified, is fed into an oscilloscope and recorded.

Three thin film gauges were used for the measurement of the shock wave speed. Each one of them was mounted in one of the instrumentation station ports, provided for that purpose, as shown in Figure 1.

Calibration of these gauges was not necessary because the signal obtained from them, was used to trigger the oscilloscope and from their stepwise signal, time resolution was obtained which allowed determination of the shock speed.

Heat transfer thin film gauges

This type of gauge is the same as the one described above. A different name is used for purpose of identification since its intended

use is different. The principle of operation is the same as the one described for the temperature-sensitive resistance detectors and the manufacture process was done in the same manner. This gauge is located on the end plate of the Driven end of the shock tube, mounted flush with the interior surface of the plate and held in place by means of a phenolic plug of similar construction to the one shown in Figure 4. The gauge measures the temperature of the end wall before and after the arrival of the shock wave. The signal produced by the gauge is fed into an oscilloscope and is recorded photographically.

It was necessary to calibrate the heat transfer gauge in order to establish the temperature coefficient of resistivity (α). The calibration was done by placing the heat transfer gauge into a bath of ice water and recording the initial gauge temperature and resistance; the water was then slowly heated to a temperature approximately of 90°C, and readings of temperature and resistance of the gauge were recorded during the process. The following relationship^{[1],[2]} was used:

$$R_F = R_O [1 + \alpha(T_F - T_O)]$$

where

R_F = gauge resistance

T_F = gauge temperature

R_O = cold gauge resistance

T_O = initial temperature

The temperature coefficient of resistivity (α) was obtained by plotting the change in resistance versus the change in temperature.

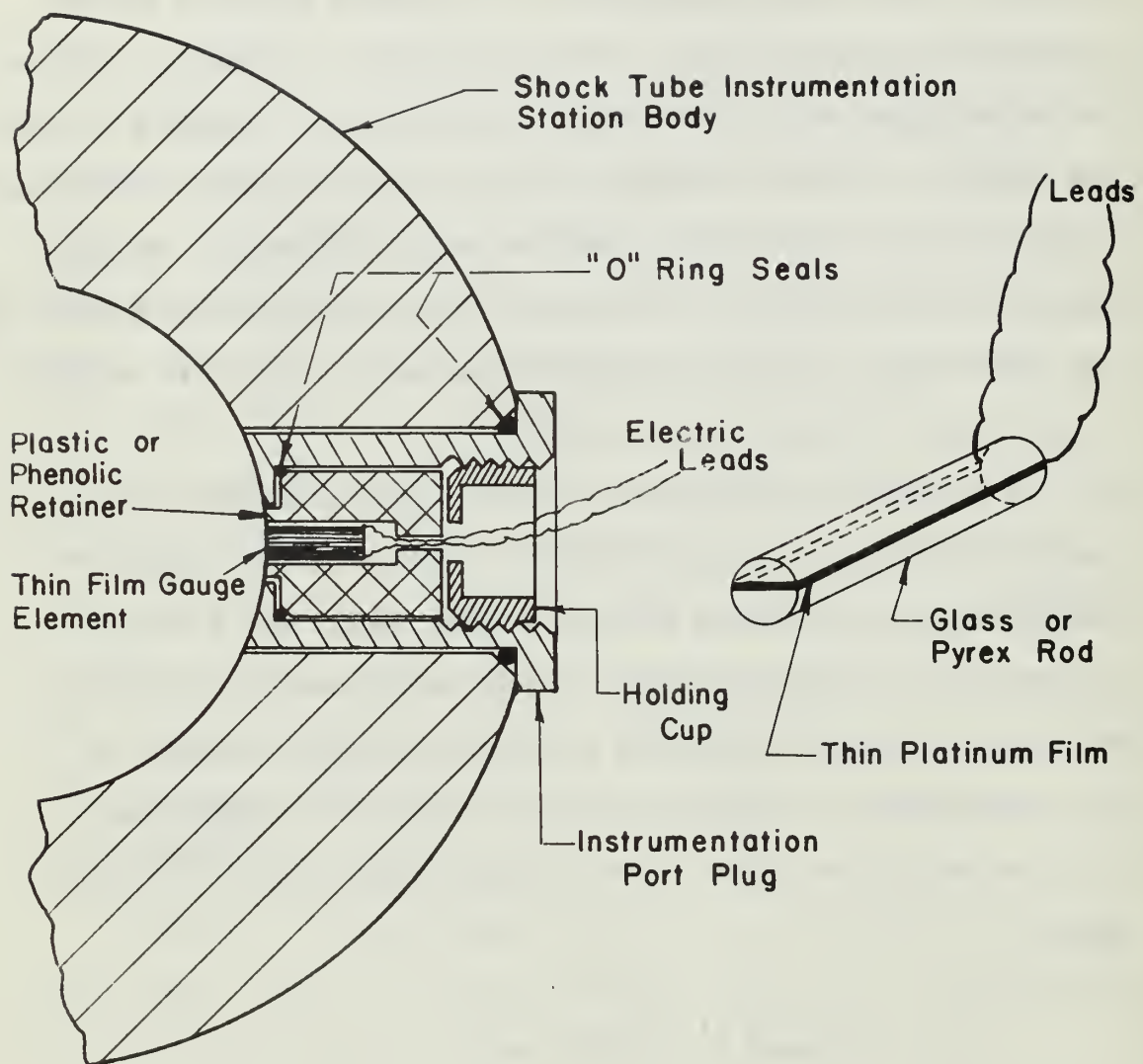


FIGURE 4

THIN FILM GAUGE ARRANGEMENT

The resistance of the thin film gauge was approximately 100 ohms, and was found to be a linear function of its temperature. Several runs were made for the calibration and one example is given in Figure 5. The plot was fitted using the least squares method. The temperature coefficient of resistivity was found to be 0.00104 ohm/ohm deg. C.

Electronics

In Figure 6 is shown a schematic of the electronic set-up used in the shock tube. Gauges Nos. 1, 2, and 3, represent the thin film gauges used for the measurement of temperature difference at the end wall. The gauges are connected to a bridge as shown in Figure 7. Since the resistances R_1 , R_2 , R_3 and R_4 are much larger than R_F , the current I through the gauge is maintained steady, thus as the change in gauge resistance is attained with the passing of the shock front, a stepwise signal in voltage is produced and this signal fed into the oscilloscopes. In the arrangement shown in Figure 6, the signal from gauge No. 1, goes to an Amplifier where it is amplified about two hundred times and from there, is used to trigger both oscilloscopes. The output from gauges No. 2 and 3 are connected to a dual beam oscilloscope, where the distance between the two peaks in their traces, gives the time delay needed to compute the shock wave speed. The output signal from the H.T. gauge is connected to the second single beam oscilloscope. The electronic equipment used is a Wide band Differential D.C. Amplifier Model 885, manufactured by Astrodata, Inc., Anaheim, California; a Type 551 Dual Beam Oscilloscope and a Type 549 Storage Oscilloscope, both manufactured by Tektronic, Inc., Portland, Oregon.

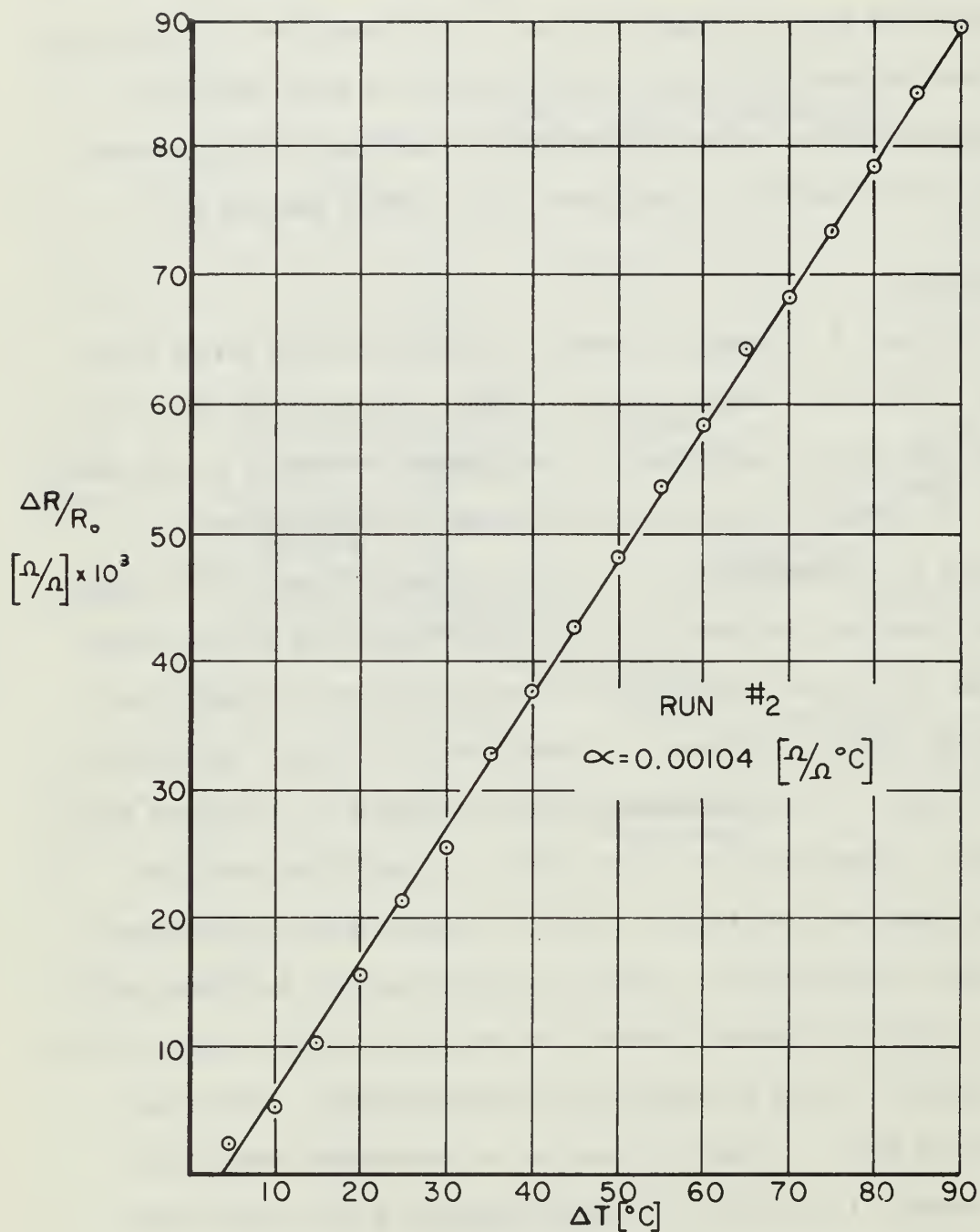


FIGURE 5
TEMPERATURE COEFFICIENT OF RESISTIVITY (α)
FOR HEAT TRANSFER THIN FILM GAUGE

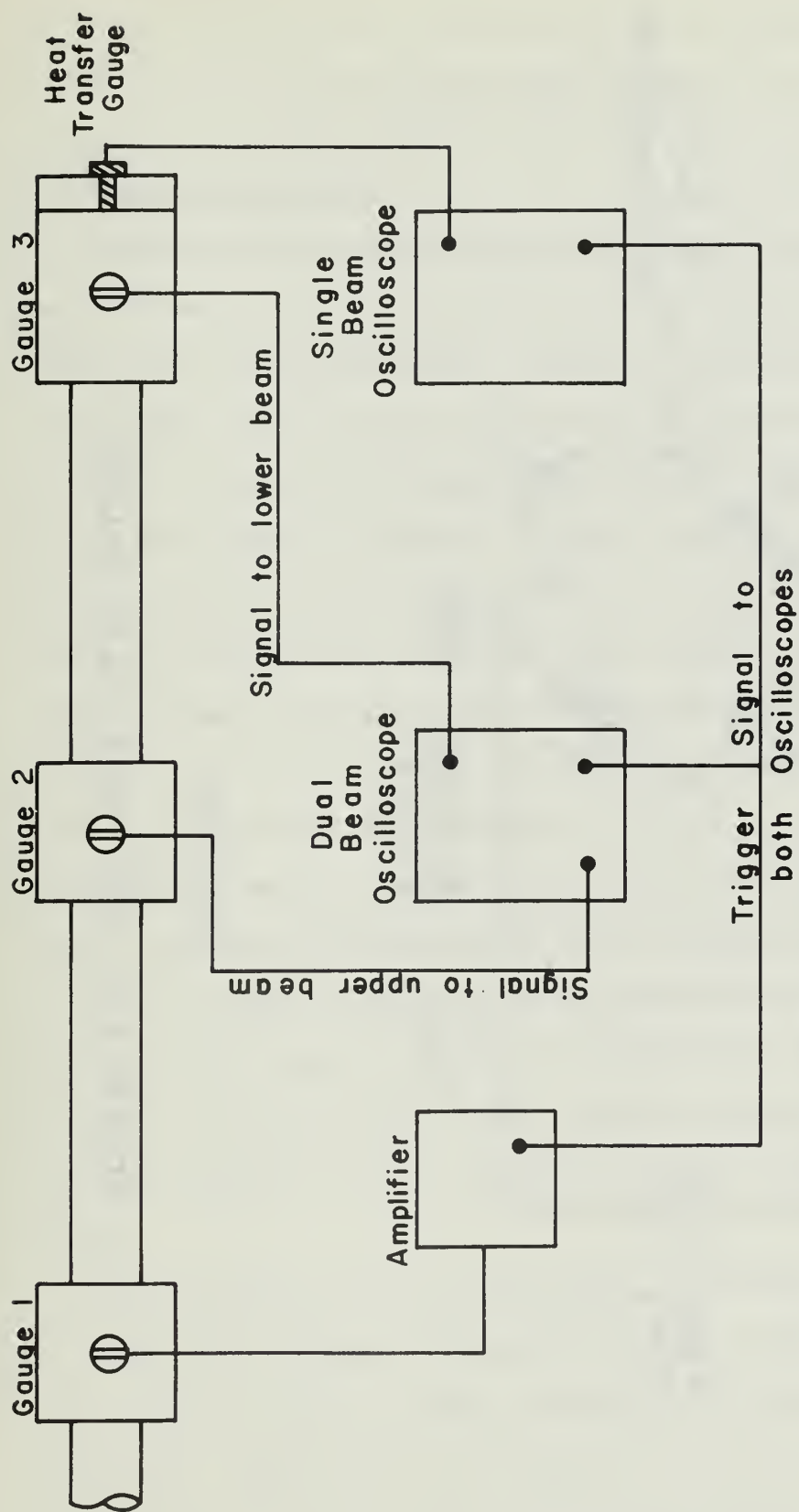


FIGURE 6
SCHEMATIC OF ELECTRONIC ARRANGEMENT

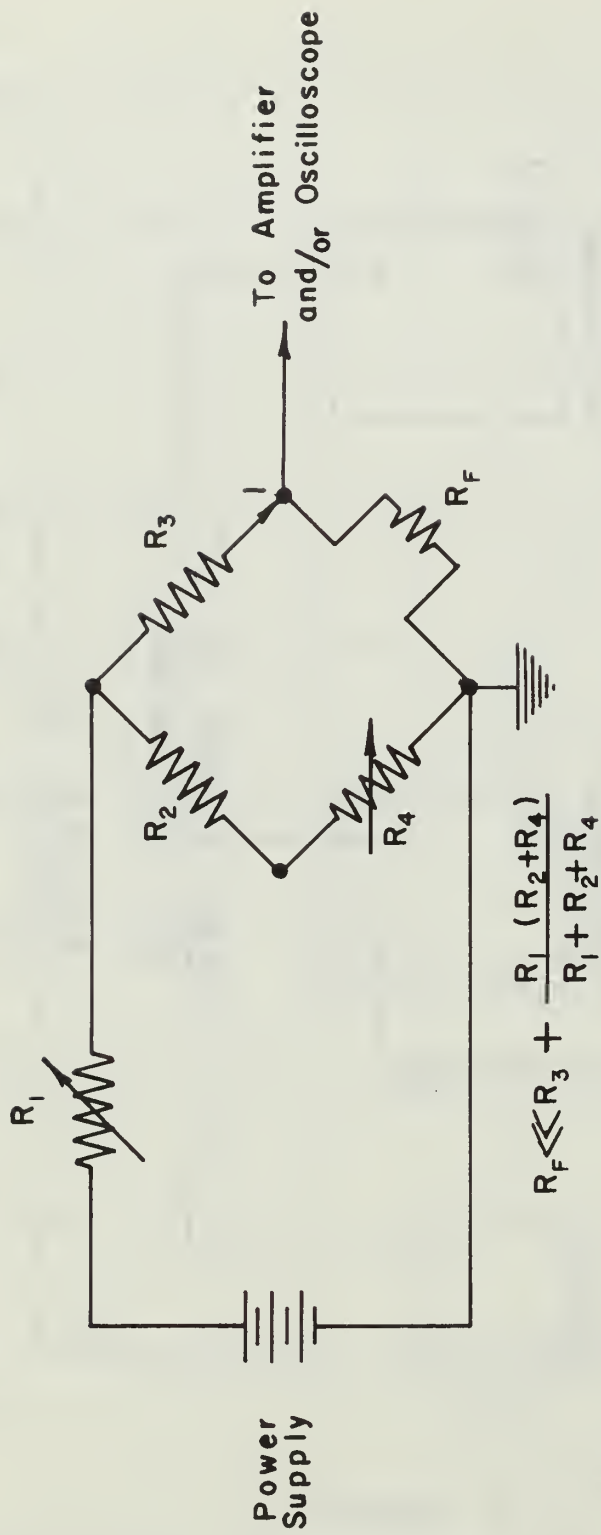


FIGURE 7

SCHEMATIC FOR THIN FILM GAUGES

III. OPERATING PROCEDURES

Filling and Vacuum System

The first step in operating the shock tube, is to obtain a vacuum in the Driven end. With reference to Figure 3 and starting with all valves closed, the vacuum pump is turned on, and when ready to pull down vacuum, control valve No. 2 and the Main valve are open; control valve No. 1 connecting the vacuum pump with the diffusion pump, is a two-way valve, which in the open position, closes the line to the diffusion pump. Working in that condition it is possible to obtain a vacuum of approximately 10^{-3} mm. of mercury; readings are obtained from either the vacuum gauge and/or thermocouple gauges. If a higher vacuum is needed, the diffusion pump is used and one opens the vacuum slide valve and close control valves No. 1 and 2. In this condition the system is operated until the desired vacuum is obtained. Although it was not tested during the present work, with the diffusion pump it is possible to obtain vacuums in the neighborhood of 10^{-9} mm. of mercury. When the desired vacuum is obtained, the main valve is closed and then, by means of the quick acting filler valve the working gas is pumped into the Driven end. The gas is usually stored in high pressure bottles.

The next step is to fill the Driver end with the gas to be used, to the desired pressure. A vacuum pump could be used in the driven end, in order to assure a clean and moisture free atmosphere before the working gas is admitted. With reference to Figure 2, the gas, usually stored in high pressure bottles, is fed into the driver section, by

means of the pressure control valve and at the same time to the diaphragm chamber. Assuming a pressure P_4 is desired in the driver end, the diaphragm chamber is filled up to a pressure P_4' less than P_4 . The chamber, actually a very small compartment of the tube in length, is sealed off by two diaphragms, the first being thick enough to withstand the pressure difference $P_4 - P_4'$ and the second one to withstand the pressure P_4' but not P_4 . When the required pressure has been reached in the driver section, the diaphragm chamber is either rapidly evacuated or expanded and the two diaphragms are then burst almost at the same time. This rather simple method of rupturing the diaphragm has the main advantage of giving a precise control pressure at which the diaphragms are ruptured and permits firing of the tube at the desired moment. This ability to control the firing of the tube is highly desired if for any reason something went wrong with the electronics and data recording equipment at the last moment.

To evacuate the shock tube after it has been fired, bleed valves are provided along the sections of the tube as indicated in Figures 2 and 3.

Data recording

The successful run of the experiments depends entirely in the ability of recording the required data. Due to the short time every shot lasts, the low output signals of the thin film gauges and the high sensitivity of the equipment to be used, this part of the experiment required some coordination of the many factors involved.

The data recorded was the following: driver end pressure, driven end pressure, initial temperature in the shock tube, time

required for shock waves to travel a fixed distance and voltage rise in the end wall at shock arrival. The first three measurements were taken by direct reading of the instruments provided for that purpose. The time required for the shock wave to travel a fixed distance in the shock tube, namely the distance between thin film gauges No. 2 and 3 [Figure 6] was obtained by means of a dual beam oscilloscope and recorded using a Polaroid film. A typical trace of the signal obtained is shown in Plate 4. With above data, the speed of the shock wave was determined and knowing the speed of sound in the gas used^[2] the shock wave Mach number was computed.

The temperature rise in the end plate is given by the following relationship:

$$\Delta T = T_w - T_o = \frac{\Delta E}{\alpha \times I_o \times R_o}$$

The temperature coefficient of resistivity (α) was previously determined for the gauge as described before; the current (I_o) and resistance (R_o) were measured before the runs. The change in voltage was recorded from the oscilloscope hook to the heat transfer thin film gauge shown in Figure 6. A typical trace of the signal obtained is given in Plate 5.

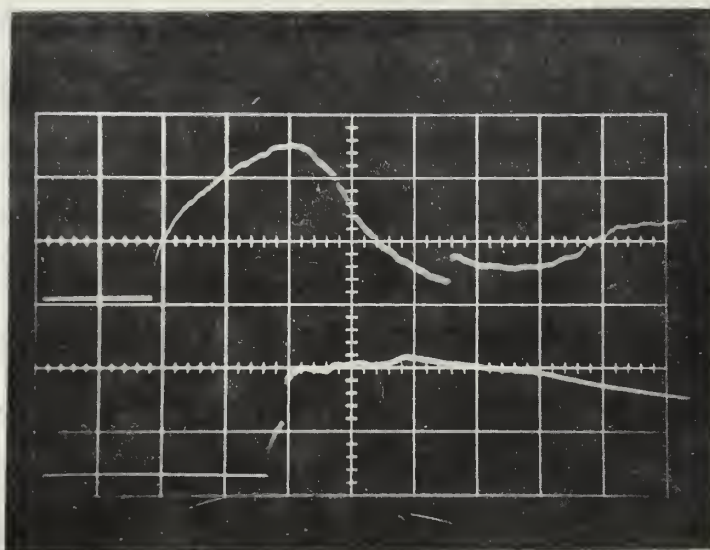


PLATE 4

TRACE OF TEMPERATURE SENSITIVE
RESISTANCE DETECTORS

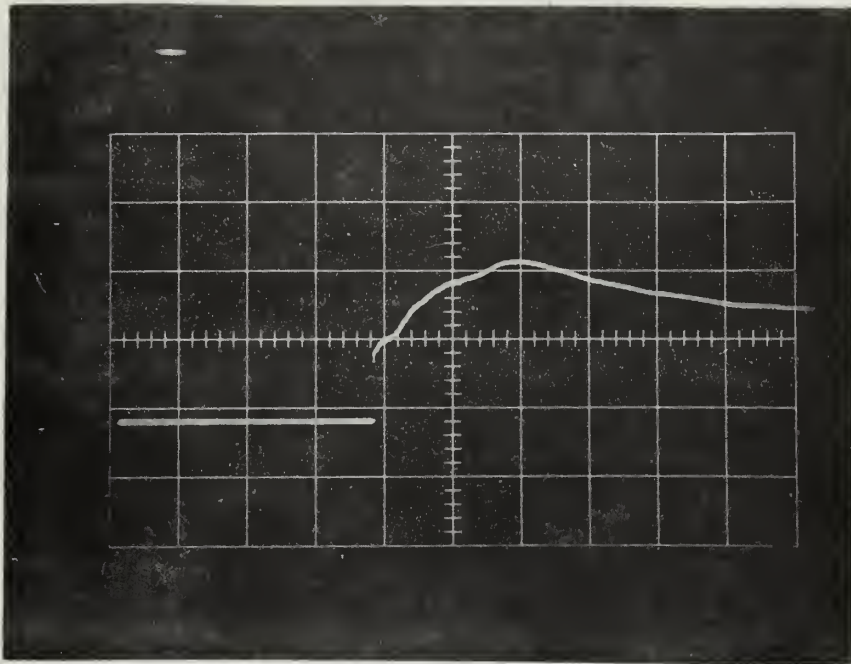


PLATE 5

TRACE OF HEAT TRANSFER THIN FILM GAUGES

CHAPTER III

THEORY BEHIND SHOCK TUBE OPERATION

I. GENERAL THEORY

The theory of the shock tube is well known and clearly described in many textbooks. The same comment can be made in regard to the theory of shock waves. It is not the intended purpose of this thesis to go deeply into the deviation of the different relations governing the actual phenomenon occurring in the tube, but to give a simple presentation on the production of a shock wave and then look in more detail at the theory governing the experiment which was performed.

In Figure 8 is shown the thermodynamic history of the shock tube. Figure 8a and 8b corresponds to time $t_0 = 0$. The Driver end corresponds to region (4) and the Driven end to region (1). At $t_0 = 0$ the temperature of both regions is the same.

At the appropriate time the diaphragm is broken. A shock wave (S) is propagated into the driven end and a rarefaction (or expansion) wave (R) is propagated back into the driver end. This is shown in Figure 8c at time $t_1 > 0$. As the shock front travels into region (1), the fluid is compressed to a higher pressure P_2 (Figure 8d) and higher temperature T_2 (Figure 8e) in a nonisentropic process. On the other hand, as the rarefaction wave travels into region (4), the fluid is expanded to a lower pressure P_3 and a lower temperature T_3 by a process which is essentially isentropic. Thus, although the pressures P_2 and P_3 are equal, there are two regions between (R) and (S). These two regions correspond to regions (2) and (3) in the graphs of Figure 8. The gas in region (2)

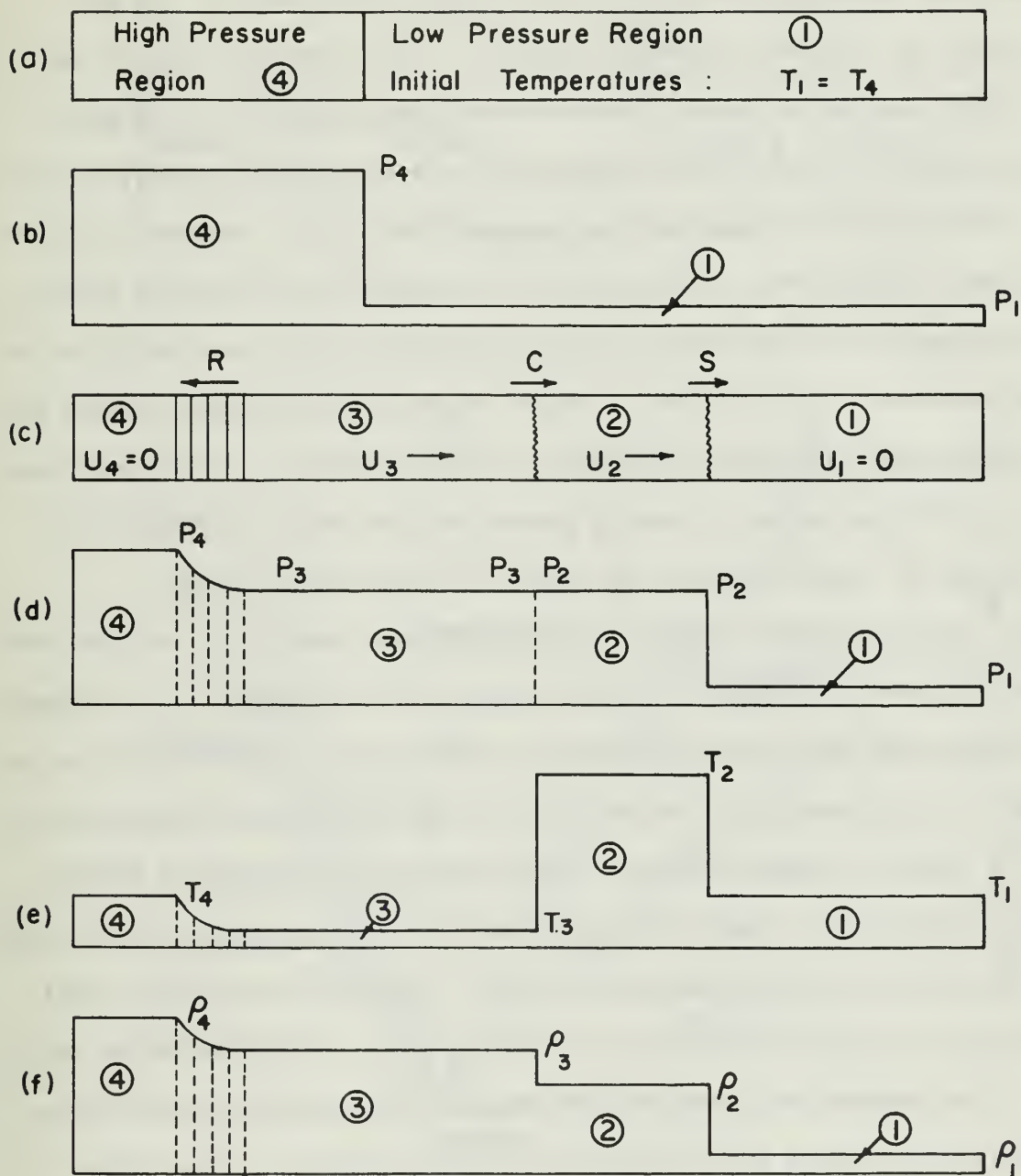


FIGURE 8
THERMODYNAMIC HISTORY OF THE
SHOCK TUBE

has been compressed and heated by the shock wave, however, the gas in region (3) has been expanded and cooled. The narrow zone called the contact surface or contact discontinuity indicated by (C) in Figure 8c represents the line where a temperature and density discontinuity exists, although pressures are the same on each side of (C). Physically it denotes the position occupied by that gas which was originally at the diaphragm and is the point where the experimental gas and the driver gas make contact. This "contact surface" travels along the tube behind the shock front. The above explanation is the ideal one. In the real case some mixing of gases is usually present at the contact surface which causes the temperature drop to occur in a finite time period.

The most common notation for the different regions is the one used in the above explanation. Another region, called region (5), is present in the shock tube operation where the shock wave is reflected at the end wall of the tube with a further rise in temperature and pressure exists. This region is shown in Figure 9, which actually represents a physical plot (distance vs time) of the phenomenon initially produced in the shock tube after the diaphragm has been burst. It can be seen in this plot, that the rarefaction (or expansion wave) covers a zone characterized by falling temperature, pressure and density below the initial conditions. These waves spread with time and the fluid properties changes occur in a more gradual process as compared with the shock front and contact surface. Due to their spreading action, these waves are called the expansion fan, with the initial and terminal wave called the head and tail waves respectively.

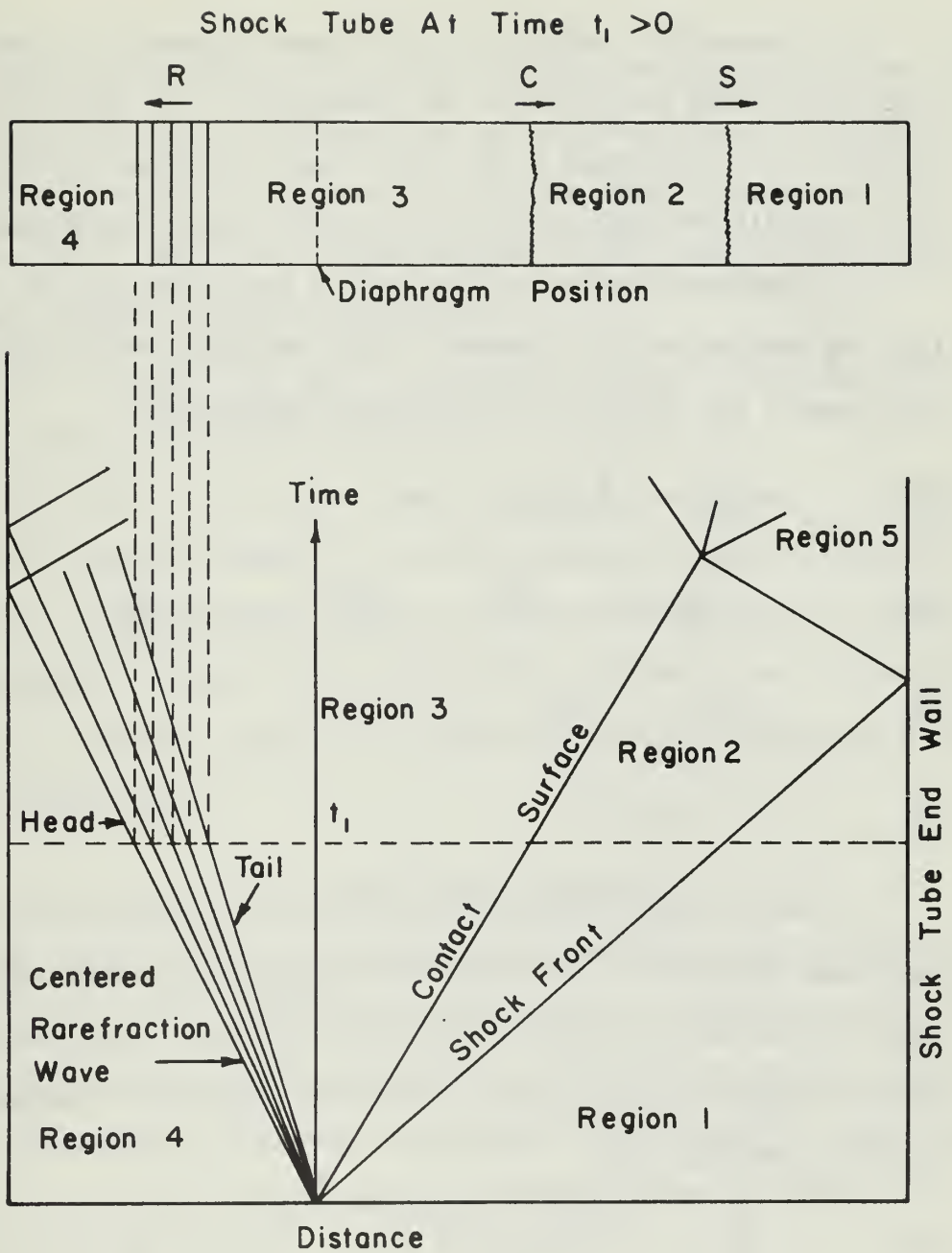


FIGURE 9

PLOT OF DISTANCE VS. TIME IN SHOCK
TUBE AFTER DIAPHRAGM IS BROKEN

The theoretical analysis for shock tube phenomenon is greatly simplified by the assumption of one-dimensional flow, where the flow properties are considered to be uniform over any cross-section and to vary only with distance along the tube and in general with time.

The fundamental equations governing a non-stationary one-dimensional flow are the continuity, momentum, energy and equation of state and they are given by the following relationships respectively:

$$(1) \quad \frac{\partial \rho}{\partial t} + \frac{\partial}{\partial x} (\rho u) = 0$$

$$(2) \quad \rho \frac{\partial u}{\partial t} + \rho u \frac{\partial u}{\partial x} = - \frac{\partial p}{\partial x} = - a^2 \frac{\partial \rho}{\partial x}$$

$$(3) \quad \frac{\partial s}{\partial t} + u \frac{\partial s}{\partial x} = 0$$

$$(4) \quad p = p(v, T)$$

The most common procedure to solve for the relationships applied to shock tube operation is using the above equations together with the methods of characteristics. A detailed coverage of these derivations is given in Reference [1] and [2], and for the method of characteristics itself in Reference [9].

$$(5) \quad \frac{p_4}{p_1} = \frac{2\gamma_1 M_1^2 - (\gamma_1 - 1)}{\gamma + 1} \left\{ 1 - \frac{\gamma_4 - 1}{\gamma_1 + 1} \times \frac{a_1}{a_4} \left(M_1 - \frac{1}{M_1} \right) \right\} - \frac{2\gamma_4}{\gamma_4 - 1}$$

$$(6) \quad \frac{p_5}{p_1} = \left\{ \frac{2\gamma M_1^2 - (\gamma - 1)}{\gamma + 1} \right\} \left\{ \frac{(3\gamma - 1)M_1^2 - 2(\gamma - 1)}{(\gamma - 1)M_1^2 + 2} \right\}$$

$$(7) \quad \frac{T_5}{T_1} = \frac{\{2(\gamma - 1)M_1^2 + (3 - \gamma)\} \{(3\gamma - 1)M_1^2 - 2(\gamma - 1)\}}{(\gamma + 1)^2 M_1^2}$$

Equation (5) relates the initial applied pressure ratio across the diaphragm to the shock wave Mach number. It gives a measureing of the strength of the shock in a given test gas and shows how for a given pressure ratio, the shock strength depends on the specific-heat ratio and sound speed in the high pressure gas.

The strongest shocks can be obtained by using a driver gas having a high speed of sound and low specific heat ratio.

Equations (6) and (7) are useful to determine the state of the gas behind the reflected shock. In the form presented they are specially suited for the experiment, leading to a full solution of the pressure and temperature behind the reflected shock in terms of the incident Mach number and initial pressure and temperature, parameters measured directly from the experiment.

II. THEORY FOR EXPERIMENTS

The region behind the reflected shock wave (region 5) is idealized to consist of a hot semi-infinite gas adjacent to a semi-infinite solid. Viscouse dissipation may be neglected and the pressure assumed constant in the gas boundary layer near the end wall of the tube^[6]. Under these conditions, we may write the equations of continuity and energy as

$$(8) \quad \frac{\partial \rho}{\partial t} + \frac{\partial}{\partial x} (\rho u) = 0$$

and

$$(9) \quad \rho c_p \left(\frac{\partial T}{\partial t} + u \frac{\partial T}{\partial x} \right) = \frac{\partial}{\partial x} \left(k \frac{\partial T}{\partial x} \right)$$

The continuity equation is satisfied by introducing a stream function ψ , such that:

$$(10) \quad \frac{\rho}{\rho_w} = \frac{\partial \psi}{\partial x}, \quad \frac{\rho u}{\rho_w} = - \frac{\partial \psi}{\partial t}$$

Changing coordinates from x to ψ , the energy equation becomes:

$$(11) \quad \frac{1}{\alpha_w} \left(\frac{\partial \theta}{\partial t} \right)_{\psi} = \frac{\partial}{\partial \psi} \left(\frac{K(\theta)}{\theta} \times \frac{\partial \theta}{\partial \psi} \right)$$

where

$$(12) \quad \alpha_w = \frac{k_w}{\rho_w c_p}, \quad \theta = \frac{T}{T_w}, \quad K(\theta) = \frac{k}{k_w}, \quad \frac{\rho}{\rho_w} = \frac{T_w}{T}$$

With the above transformation, no characteristic time appears in the equation, leaving θ as a function of the expression $\frac{\psi^2}{\alpha_w t}$, implying that the wall surface temperature, T_w , is a constant.

Introducing a similarity parameter

$$(13) \quad \eta = \frac{\psi}{(2\alpha_w t)^{1/2}}$$

The one dimensional time dependent energy and continuity equations near the end wall of the tube reduce to

$$(14) \quad \frac{d}{d\eta} \left(\frac{K(\theta)}{\theta} \times \frac{d\theta}{d\eta} \right) + \eta \frac{d\theta}{d\eta} = 0$$

subject to the following boundary conditions:

$$(15) \quad \theta(0) = 1.0, \quad \theta(\infty) = \frac{T_{\infty}}{T_w}$$

The subscripts w and ∞ refer to numerical values evaluated at the end wall condition just after the shock wave arrival and to any quantity measured behind the reflected shock wave, respectively.

Equation (14) can be integrated from $\eta = 0$ to $\eta = \infty$, after the temperature dependence of the thermal conductivity is established. Reference [5] and [6] assume the thermal conductivity to vary as a power law in temperature

$$(16) \quad \frac{k}{k_w} = \left(\frac{T}{T_w} \right)^a$$

With that assumption, equations (14) and (15) can be used to obtain the following relations:

$$(17) \quad \theta_\infty = \frac{T_\infty}{T_w} = f(a, q_w), \quad q_w = \left(\frac{d\theta}{d\eta} \right)_{\eta=0}$$

By equating the heat flux at $x = 0$ to the heat flux at the surface of the solid end wall it can be shown^[5] that

$$(18) \quad q_w = \sqrt{\frac{2}{\pi}} \lambda \frac{T_w - T_s}{T_w}$$

where

$$(19) \quad \lambda = \frac{\beta_s}{\beta_w} = \left(\frac{k_s \rho_s c_s}{k_w \rho_w c_p} \right)^{1/2}$$

In the above equations, the subscripts s and w refer to properties of the gauge and properties of the gas at the wall temperature respectively.

Since the quantities θ_{∞} and q_w can be experimentally evaluated from each run, a series of tests yields an experimental relation between them for the gas tested. Equation (16) established that the relation of these quantities is dependent on the exponent a . Then, by comparing the theoretical and experimental data it is possible to choose a value of " a " which best fits the data. The numerical value of " a " was computed by minimizing the sum of the squares of the deviation between the experimental and theoretical curves. Once it was established, the temperature dependence of the thermal conductivity is given by equation (16).

IV. EXPERIMENTAL RESULTS AND DISCUSSION

I. DESCRIPTION OF EXPERIMENT

Purpose

The purpose of the experiment described herein was to look at the thermal conductivity of argon at relatively higher pressure, i.e. 10 to 50 atmospheres and to compare the results obtained with those similar experiments, done at/or around atmospheric pressure. Previous data for experiments having the same conditions of the one done for this thesis was not available, so a comparison in that sense was not possible.

Calibration Runs

With reference to the theory and equations presented in the previous chapter, it was necessary to calibrate the thin film heat transfer gauge to obtain a value of β_s , in order to compute later the experimental values of q_w . This calibration was done in the shock tube, by making a series of runs (30 in total), where argon was heated to temperatures ranging from 1000 to 1500 degrees Kelvin. In this range of temperature, the thermal conductivity of argon has been experimentally determined. To determine the heat transfer rate q_w , a value of the parameter "a" is required. The value $a = 0.697$ taken from Collins and Menard^[6] was used. Equation 18 was then used to obtain a value for $\beta_s = 0.062060 \text{ cal/cm}^2 \text{ deg. K (sec)}^{1/2}$ with a standard deviation of ± 0.010 . This value was found to be around 15% higher than others previously determined. Due to this reason, and that the

calibration runs were accomplished also at relatively high pressures, between 1 and 10 atmospheres, the validity of the use of the parameter $a = 0.697$ is questionable. Unfortunately, due to lack of time it was not possible to go into the determination of the optimum value of "a" to be used in this case.

Experimental Runs

The experimental runs were made in the shock tube previously described using the data recording equipment and instruments mentioned before. The gas tested was Argon using Helium as a driver. The runs were made, as to obtained temperatures between 1500° to 5000°K and pressures of 10 to 50 atmospheres in the region behind the reflected shock wave (region 5). In the determination of thermal conductivity, the value of k_w was obtained from the values given in Cook^[8]. Thus the problem was reduced to find a value of "a" for equation (20) to fit the data.

$$(20) \quad K(\theta) = \frac{k}{k_w} = \theta^a$$

A list of data recorded, as well as the values computed is given in Plate 6.

II. DATA REDUCTION

For every run made, the data obtained was the driven end pressure (p_1), the shock tube temperature (T_0), the time resolution for the shock wave mach number computation and the voltage rise at the end wall thin film heat transfer gauge, used for computations of temperature rise in the end wall. With that data, it was then possible to obtain a

PRIN	P1	TP	DT	DE	MS	OTEMP	TS	P5	TW	OINF	QM
1	1142.4910	206.890	0.00180	0.019487	2.6266	12.2526	1673.8184	38072.7383	309.1323	5.4146	2.75182
2	1014.7390	206.890	0.00180	0.020425	2.6266	12.8361	1673.8184	33815.4609	309.7158	5.4044	3.06991
3	063.7698	207.160	0.00175	0.021562	2.7016	13.4195	1765.1057	34344.8047	310.5793	5.6833	3.17419
4	890.0000	207.160	0.00175	0.021562	2.7016	13.4195	1765.1057	32012.4766	310.5793	5.6833	3.29744
5	838.2000	207.440	0.00170	0.021875	2.7811	13.6140	1864.5298	32657.7187	311.0540	5.9942	3.30459
6	787.1460	207.440	0.00165	0.021875	2.8654	13.6140	1971.2415	33228.8359	311.0540	6.3373	3.27370
7	738.0000	207.720	0.00165	0.022500	2.8654	14.0030	1973.0974	31095.0621	311.7229	6.3297	3.40317
8	697.0600	207.720	0.00160	0.023125	2.9549	14.3920	2090.0117	31471.9922	312.1118	6.6964	3.55255
9	636.2098	207.720	0.00155	0.023750	3.0502	14.7800	2218.3479	31674.7500	312.5007	7.0987	3.63168
10	584.2000	208.000	0.00150	0.024375	3.1519	15.1699	2361.8860	31660.4531	313.1697	7.5419	3.72063
11	533.3000	208.000	0.00145	0.025000	3.2606	15.5599	2518.1453	31526.8477	313.5588	8.0309	3.82026
12	485.0300	208.000	0.00145	0.025000	3.0502	15.5599	2220.4343	26680.1328	313.5588	7.0814	4.17829
13	441.3200	208.000	0.00145	0.025000	3.2606	15.5599	2518.1453	28449.2227	313.5588	8.0309	4.03725
14	432.4340	208.160	0.00142	0.025312	3.3178	15.7534	2603.7122	26711.5508	313.8931	8.2949	4.22359
15	382.2408	208.280	0.00137	0.026250	3.4385	16.3368	2787.7539	25829.7891	314.6165	8.8608	4.44940
16	355.3659	208.280	0.00135	0.026250	3.4892	16.3368	2866.5920	24903.1562	314.6165	9.1114	4.53677
17	331.2158	208.550	0.00135	0.027875	3.4892	17.8927	2869.1870	23212.0920	316.4424	9.0670	5.12939
18	305.4348	208.550	0.00130	0.028750	3.6388	17.8927	3105.2180	23710.6836	316.4424	9.8129	5.07195
19	280.4609	208.550	0.00127	0.029750	3.7081	17.8927	3222.7139	22847.5078	316.4424	10.1842	5.17254
20	254.0000	208.550	0.00125	0.029062	3.7823	18.0972	3347.3118	21695.8008	316.6370	10.5714	5.37052
21	241.3000	208.550	0.00125	0.029125	3.7823	17.5037	3347.3118	20611.0117	316.0535	10.5910	5.34909
22	228.6000	208.550	0.00125	0.028750	3.7823	17.8927	3347.3118	19526.2187	316.4424	10.5779	5.61898
23	215.5700	208.000	0.00120	0.029750	3.9309	17.8927	3613.5522	20346.4609	315.8926	11.4392	5.50795
24	203.2000	208.000	0.00120	0.029687	3.9309	18.4762	3613.5522	19149.6094	316.4761	11.4181	5.86125
25	180.7540	208.000	0.00115	0.031250	4.1117	19.4456	3922.1790	19892.6328	317.4485	12.3553	6.02990
26	170.3000	207.800	0.00117	0.029375	4.2237	18.2817	3761.5596	17669.7305	316.1714	11.8972	6.05465
27	166.3700	207.720	0.00110	0.030625	4.2081	19.0596	4269.7578	19261.6719	316.7795	13.4786	6.02231
28	152.4000	207.720	0.00112	0.029375	4.2074	18.2817	4088.2854	16738.5937	316.0015	12.9376	6.23147
29	130.7000	207.720	0.00110	0.027500	4.2981	17.1148	4269.7578	16173.9259	314.9347	13.5519	5.96023
30	128.0140	207.440	0.00115	0.027500	4.1112	17.1148	3914.8076	13350.0469	314.5547	12.4456	6.59023
31	114.2000	207.440	0.00112	0.026250	4.2024	16.3368	4084.4402	12553.9414	313.7766	13.0170	6.50944
32	101.6000	205.220	0.00105	0.029375	4.5027	18.2817	4633.0898	13106.1250	313.5015	14.7785	7.13009
33	77.6700	205.520	0.00100	0.025625	4.7273	15.9478	5105.6367	11179.0547	311.8677	16.3712	6.78605
34	64.5140	206.330	0.00100	0.025625	4.7279	15.9478	5112.7109	9309.7695	312.2776	16.3723	7.44529
35	1270.0000	208.160	0.00220	0.023125	2.3639	14.3920	1385.2849	31402.9258	312.5317	4.4325	3.55225
36	1210.2000	208.160	0.00185	0.023750	2.5555	14.7809	1598.0552	37645.4180	312.9207	5.1069	3.30232
37	1140.3000	208.280	0.00185	0.024375	2.5555	15.1699	1598.8049	36076.8594	313.4495	5.1007	3.46338
38	1117.5000	208.550	0.00190	0.014375	2.4884	8.9453	1523.6702	32011.1094	307.4961	4.9551	2.21914
39	1066.1460	205.420	0.00190	0.015000	2.4884	9.3353	1523.0073	30537.8711	307.7551	4.9488	2.37339
40	977.0000	208.280	0.00185	0.015000	2.5555	9.3353	1598.8049	28626.1992	307.6150	5.1974	2.45845
41	851.5340	208.280	0.00180	0.015000	2.6266	9.3353	1681.7112	28376.7969	307.6150	5.4669	2.47001
42	762.0000	208.160	0.00165	0.021250	2.8654	13.2250	1975.8804	32167.3125	311.3647	6.3459	3.23350
43	711.2000	208.000	0.00165	0.020625	2.9554	12.8361	1974.9534	30022.8242	310.8359	6.3537	3.26262
44	660.3000	208.000	0.00170	0.017500	2.7811	10.8912	1868.0405	25730.3203	308.8911	6.0476	3.02470
45	608.7900	208.000	0.00150	0.023125	3.1512	14.3920	2361.8860	30283.9023	312.3918	7.5607	3.62392
46	500.0000	207.880	0.00145	0.022500	3.2606	14.0030	2514.9612	30025.5781	311.8628	8.0707	3.54797
47	457.2000	207.440	0.00140	0.025000	3.3771	15.5580	2686.3181	29529.5156	312.9988	8.5825	3.96399

PLATE 6
 TABULAR SOLUTION OF EXPERIMENT

dimensionless plot of $\theta_{\infty} = T_{\infty} / T_w$ vs $(d\theta/dn)_w = q_w$ for the experiment accomplished. After that was done and by using equation (14) chapter III and by comparing the theoretical with the experimental values obtained and minimizing the sum of their deviations a plot of the residuals versus "a" was obtained and from it, the best value of "a" to fit the data was selected.

In appendix I are given sample computations indicating the breakdown for equation (14) obtained in order to solve it using the IBM 360 computer of the school and for the determination of q_w for the experiments run.

Although several partial computer programs were written, Appendix II shows the final computer program written that solves for the best value of a, having as inputs the initial data obtained. The output of those programs was divided in three steps; the first, a tabular array given for each run the initial data and the computed values obtained for the mach number, temperature raise in the end wall, pressure and temperature in the region behind the reflected shock, final temperature in the end wall, a value of $\theta = T/T_w$ and a value for q_w . With these last two quantities, a subroutine called W4PLOT was used to obtain a graphical representation of the experimental results. Then, equation (14) was solved, using a subroutine called SYSZDE and from it, a theoretical value of $\theta_{\infty} = T_{\infty}/T_w$ was obtained, for different values of "a". The residuals between the theory and experiment were then obtained and these values, plotted versus a, yielded the selection of the optimum value of "a". This was represented in a graph, using again the subroutine W4PLOT. The final plot obtained is shown in Figure 10.

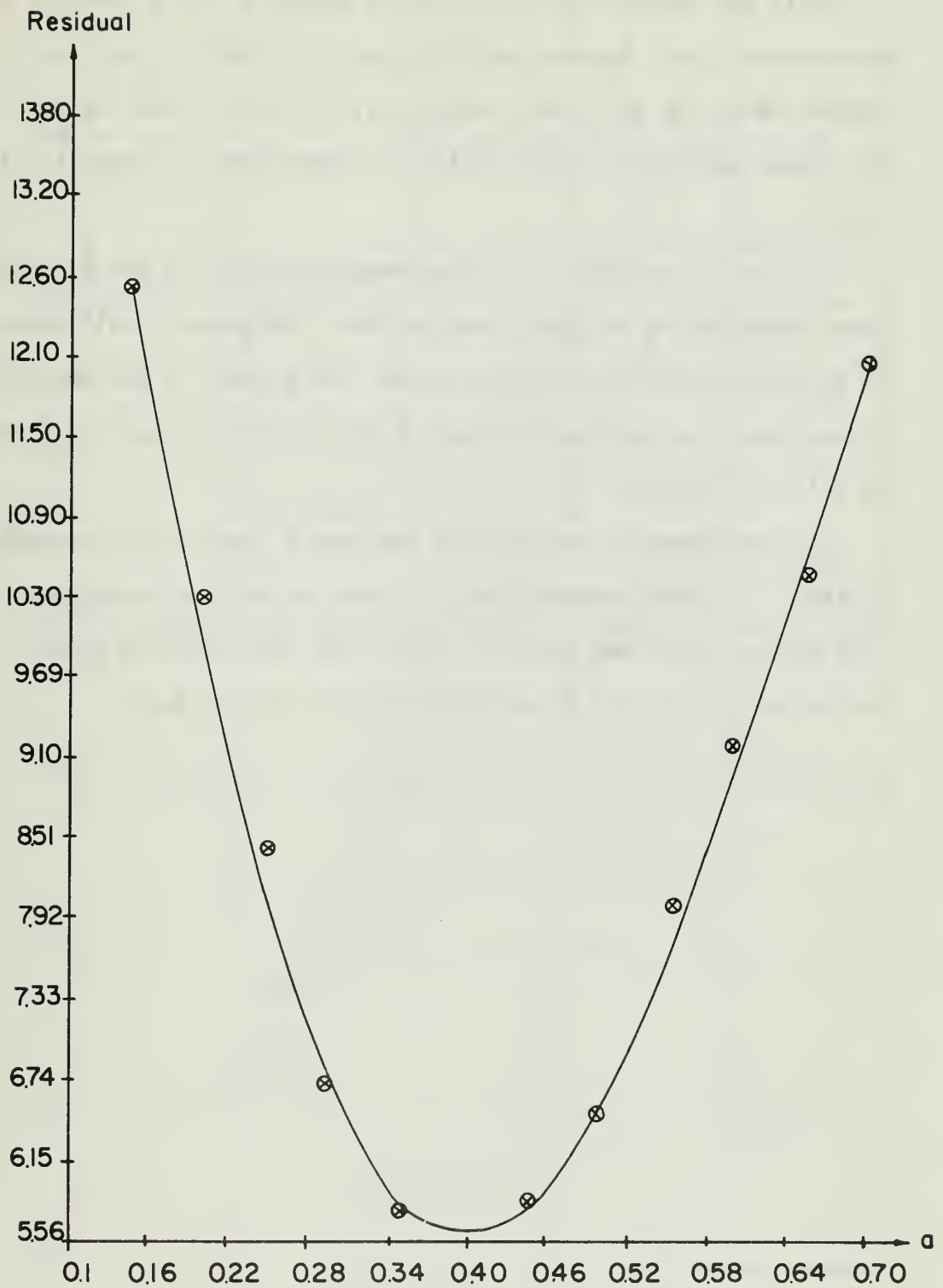


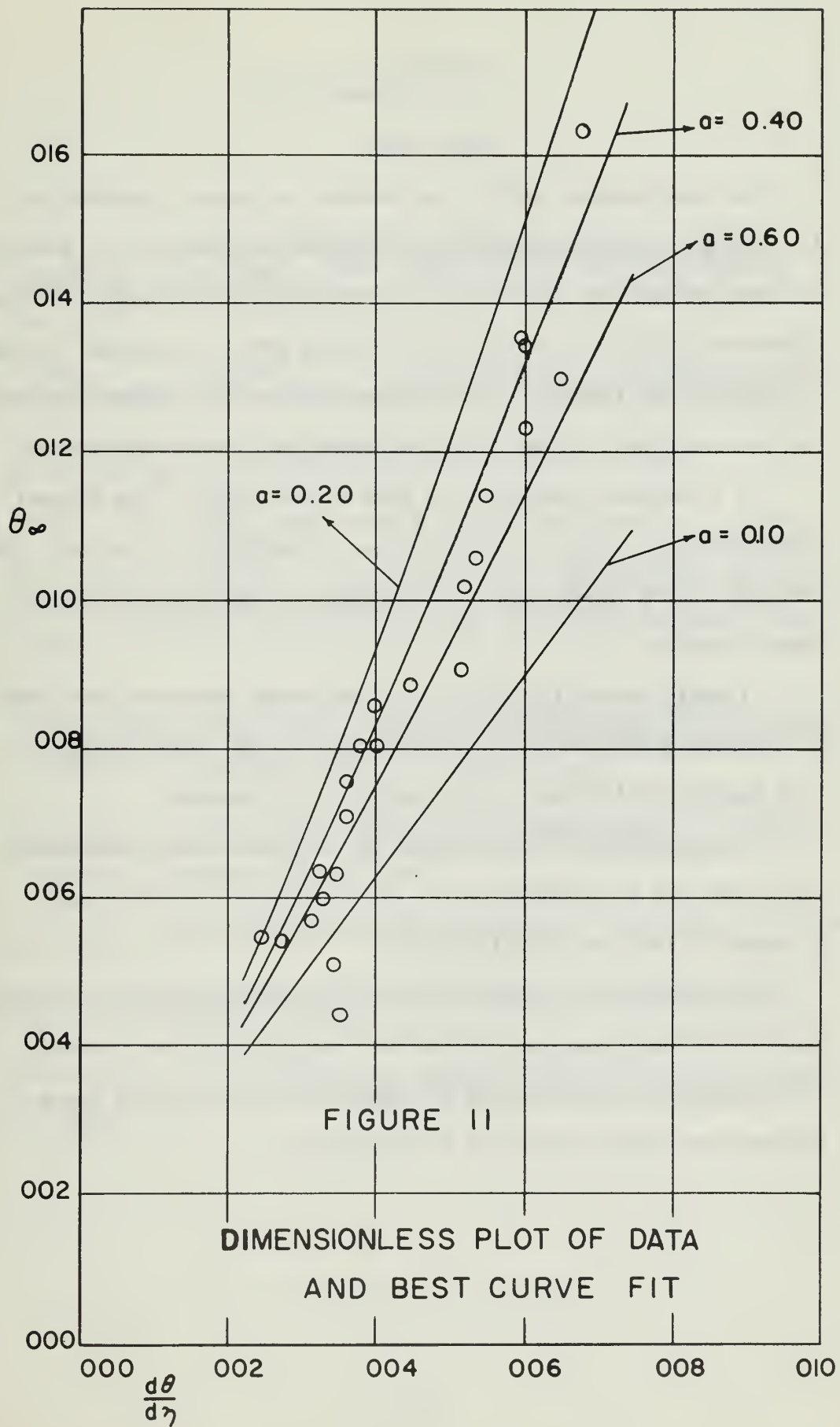
FIGURE 10

PLOT OF EXPONENT a VS. RESIDUAL

With the computer program shown in appendix III, a graph of the experimental data, together with the curve for best fit was then obtained and at the same time, theoretical curves for other values of "a" chosen arbitrarily were plotted for comparison, as shown in Figure 11.

Due to the relatively low time resolution used in the oscilloscope connected to the heat transfer thin film gauge, 1 millisecond vs 10 microseconds of reference 6, the flat plateau at the beginning of the trace, as the one mentioned in that reference, was not visible in all the pictures.

In approximately one third of the data a flat plateau was identifiable. Another reference point visible on all the traces was used. This plateau point was some 25% higher than the reference point. A correction factor of 1.25 was then used for all the data.



CHAPTER IV

CONCLUSIONS

The experimental data is preliminary in nature, nevertheless the thermal conductivity of Argon at higher pressures 10 to 50 atmospheres has been determined. In the relationship given by equation 16, the experimental value of $a = 0.4$ was obtained with k_w computed as shown in appendix II, step AKW. No previous data in this range of pressures has been obtained so that it is not possible to make comparisons.

It is necessary perhaps, in some future study of the thermal conductivity of Argon, to explain from a theoretical view point the decrease in the value of "a" with pressure, from that obtained at lower pressures.

It would appear that it is also necessary to repeat some aspects of the experiment in order to verify some of the results obtained. This applies particularly to the value of β_s obtained.

The purpose of this thesis was to develop a fully functioning shock tube and to demonstrate the functioning of the shock tube by means of an experimental problem.

The shock tube is now a working tool in the Aeronautical Engineering Department and some preliminary results have been obtained in an experiment to determine the thermal conductivity of Argon in the pressure range from 10 to 50 atmospheres.

BIBLIOGRAPHY

1. Glass, I., and Hall, J. Handbook of Supersonic Aerodynamics, Section 18, Shock Tubes, Navord Report 1488, The Johns Hopkins University Applied Physics Laboratory, Silver Spring, Maryland, Dec. 1959.
2. Gaydon, A. G. and Hurle, I. R., The shock tube in high-temperature chemical physics, Reinhold Publishing Corporation, N.Y., 1963.
3. Bradley, John N., Shock waves in chemistry and physics, John Wiley and Sons Inc., N.Y., 1962.
4. Wright, J.K., Shock tubes, John Wiley and Sons Inc., N.Y., 1961.
5. Collins, D.J., Greif, R., Bryson, A.E., Jr., Measurements of the thermal conductivity of helium in the temperature range 1600-6700 °K, Int. J. Heat Mass Transfer, Vol. 8 pp. 1209-1216, Pergamon Press, 1965.
6. Collins, D.J., and Menard, W.A., Measurement of the Thermal Conductivity of Noble Gases in the temperature range 1500 to 5000 °K, Tech. Report No. 32-903, Jet Propulsion Laboratory, California Institute of Technology, Pasadena, Calif., 1966.
7. Collins, D.J., and others, Hypervelocity Shock tube, Tech. Report No. 32-620, Jet Propulsion Laboratory, California Institute of Technology, Pasadena, Calif. 1964.
8. Cook, G.A., Argon, Helium and the rare gases, Interscience Publishers, N.Y. 1961.
9. Abbott, M.B., An introduction to the methods of characteristics, American Elsevier, N.Y. 1966.
10. Matulta, R.A., High temperature thermal conductivity of rare gases and gas mixtures, J. Heat Transfer, August 1968, Transactions of the ASME.

APPENDIX I

SAMPLE CALCULATIONS

a) Solution of equation (14) for data reduction:

$$(14) \quad \frac{d}{d\eta} \left(\frac{K(\theta)}{\theta} \frac{d\theta}{d\eta} \right) + \eta \frac{d\theta}{d\eta} = 0$$

from equation (12) Chapter III is found:

$$K(\theta) = \theta^a$$

Replacing in equation (14):

$$\theta^{a-1} \frac{d^2\theta}{d\eta^2} + \frac{d}{d\eta} (\theta^{a-1}) \frac{d\theta}{d\eta} + \eta \frac{d\theta}{d\eta} = 0$$

reducing above expression:

$$(21) \quad \frac{d^2\theta}{d\eta^2} + \frac{a-1}{\theta} \frac{d\theta}{d\eta}^2 + \eta \theta^{a-1} \frac{d\theta}{d\eta} = 0$$

Equation (21) represents a second order nonlinear differential equation.

In order to solve it, it was reduced to a system of two first order differential equations by the following transformation:

$$\text{Let} \quad x_1 = \theta, \quad x_2 = \frac{d\theta}{d\eta}$$

Then, the final equations are:

$$(22) \quad x_1' = x_2$$

$$(23) \quad x_2' = \frac{1-a}{x_1} x_2^2 - \eta x_1^{1-a} x_2$$

b) Determination of q_w for experiment runs:

The value of β_s was known to be

$$\beta_s = 0.06026 \left\{ \frac{\text{cal.}}{\text{cm}^2 \text{ K}^\circ (\text{sec})^{1/2}} \right\}$$

From equations (17), (18) and (19) Chapter II, is obtained:

$$q_w = \frac{d\theta}{d\eta} = \sqrt{\frac{2}{\pi}} \frac{\beta_s}{\beta_w} \frac{T_w - T_s}{T_w}$$

let $\Delta T = T_w - T_s$

Using equation of state for a perfect gas:

$$T_w \beta_w = T_w \sqrt{k_w \rho_w c_p} = T_w \sqrt{\frac{k_w P_w c_p}{R T_w}} = \sqrt{k_w P_w T_w \frac{c_p}{R}}$$

For above expression, the following holds

$$P_w = P_\infty \text{ in units of } [\text{cal/cm}^3]$$

$$k_w \text{ is given in units of } \left[\frac{\text{cal}}{\text{cm}^\circ \text{K sec}} \right]$$

$$T \text{ is given in } [^\circ \text{K}]$$

$$P = (P \text{ mm Hg}) (3.184 \cdot 10^{-15} \frac{\text{cal/cm}^3}{\text{mm Hg}}) \text{ is a conversion factor}$$

$$\frac{c_p}{R} = 2.5 \text{ for Argon}$$

Then:

$$q_w = \frac{d\theta}{d\eta} = \frac{\sqrt{\frac{2}{\pi}} \times \Delta T \times \beta_s}{\sqrt{2.5 \times k_w \times T_w \times P_\infty}}$$

A P P E N D I X I I

COMPUTATION OF EXPERIMENTAL DATA AND DETERMINATION OF EXPONENT 'A'

```
//PEN41227 JOB (1227,01ET), 'FEDERICO A. PENARANDA', MSGLEVEL=1, CLASS=1
//EXEC FORTCLG, TIME, GG=20
```

PROGRAM PURPOSE.

FOR SHOCK TUBE INVESTIGATION OF THERMAL CONDUCTIVITY IN ARGON, THE PROGRAM IS WRITTEN TO SOLVE FOR THE VALUES OF QW (REFERENCE EQ.18) AND THE RATIO OF TEMPERATURES (REFERENCE EQ.15) HAVING AS INPUTS. P1, T0, TIME RESOLUTION AND VOLTAGE RISE IN HEAT TRANSFER THIN FILM GAUGE.

THE OUTPUT FOR THE FIRST PART IS A TABULAR SOLUTION PRINTING THE RESULTS AS WELL AS THE INITIAL DATA.

AFTER THE PARAMETERS QW AND THETA INFINITE HAS BEEN COMPUTED, THE SUBROUTINE W4PLOT IS USED TO GIVE A GRAPHICAL REPRESENTATION OF THE EXPERIMENT.

THEN, USING SUBROUTINE SYS2DF, EQUATION 14 IS SOLVED FOR DIFFERENT VALUES OF THE EXPONENT 'A'. A COMPARISON BETWEEN THE EXPERIMENTAL AND THEORETICAL VALUES IS DONE AND THE RESIDUALS PLOTTED VS. THE EXPONENT 'A', YIELDING TO THE SELECTION OF 'A' THAT MINIMIZES THE RESIDUALS. THE OUTPUT IS GRAPHICALLY OBTAINED USING ONCE MORE THE SUBROUTINE W4PLOT.

```
DIMENSION X(54), Y(54,1), ERRSQ(47,13), SQRT(13,1), XA(13),
*T(50), X1(50), X2(50)
EXTERNAL X1DCT, X2DCT
N = 0
WRITE(6,103)
103 FORMAT(1H1, T2, 'RUN', T14, 'P1', T27, 'T0', T38, 'DT', T48, 'DE', T59, 'MS',
*T67, 'DTMP', T80, 'T5', T93, 'P5', T104, 'TW', T113, 'CINF', T126, 'QW', //
*///)
CC READ(5,101) NR, P1, T0, DT, DE
101 FORMAT(12,8X, F20.0, 3F10.0)
DE = DE#1.25
SMS= 151.765/(32100.*DT)
DTMP= DE/ .0016068
```



```

P5 = P1*((15.*SMS**4-R.*SMS**2 +1.)/(2.*SMS**2 +6.))
T5 = T0*((13.*SMS**4 +2.*SMS**2 -1.)/(4.*SMS**2))
TW = DTEMP+T0
OINF= T5/TW
DELP1=4.27+(0.0093*P5/760.)
DELP2=4.62+(0.0093*P5/760.)
DELPM=(DELP1+DELP2)/2.
AKW=DELPM+0.0138*(TW-310.5)
QW=1704.16970*DTEMP/(AKW*P5*TW)**0.5
N=N+1
X(N)= QW
Y(N,1)= OINF
WRITE(6,102) NR,P1,T0,DT,DE,SMS,DTEMP,T5,P5,TW,OINF,QW
102 FORMAT(15,F14.4,F12.3,F10.5,F11.6,2F10.4,2F13.4,2F10.4,F11.5,/)
IF(NR.LT.57) GO TO 99
CALL W4PLOT(X,Y,N,47,1,0,XMIN,XMAX,YMIN,YMAX)
TI=0.0
XI=1.0
H=0.01
KI=10
DO 1000 CORRESPONDS TO TOTAL NO. OF RUNS
DO 1000 J=1,47
X2I = X(J)
DO 2000 CORRESPONDS TO VARIATION OF EXPONENT A
DO 2000 K=1,13
A = 0.1 + (K-1) * 0.05
CALL SYS2DE(X1DOT,X2DOT,50,TI,X1I,X2I,T,X1,X2,H,KI,A)
ERR=X1(50) - Y(J,1)
ERRSQ(J,K) = ERR**2
CONTINUE
CONTINUE
DO 3000 K = 1,13
SUM = 0.0
DO 4000 J = 1,47
SUM = SUM + ERRSQ(J,K)
SQRT(K,1) = SORT(SUM)
CONTINUE
CONTINUE
DO 5000 K = 1,13
XA(K) = 0.1 + (K-1)*0.05
CONTINUE
CALL W4PLOT(XA,SQRT,13,13,1,0,XMIN,XMAX,YMIN,YMAX)
STOP
END

```



```

SUBROUTINE SYS2DF (F,G,N,XI,YI,ZI,X,Y,Z,H,K,A)
DIMENSION X(1), Y(1), Z(1)
X(1)=XI
Y(1)=YI
Z(1)=ZI
DO 14 I=2,N
  U=X(I-1)
  V=Y(I-1)
  W=Z(I-1)
  DO 12 J=1,K
    S1=H*F(U,V,W,A)
    T1=H*G(U,V,W,A)
    S2=H*F(U+0.5*H, V+0.5*S1, W+0.5*T1)
    T2=H*G(U+0.5*H, V+0.5*S1, W+0.5*T1,A)
    S3=H*F(U+0.5*H, V+0.5*S2, W+0.5*T2)
    T3=H*G(U+0.5*H, V+0.5*S2, W+0.5*T2,A)
    S4=H*F(U+H, V+S3, W+T3)
    T4=H*G(U+H, V+S3, W+T3,A)
    U=U+H
    V=V+(S1+2.0*(S2+S3) + S4)/6.0
    W=W+(T1+2.0*(T2+T3) + T4)/6.0
  12 X(I)=U
  14 Y(I)=V
  Z(I)=W
END

```

```

FUNCTION X1DOT(T,X1,X2)
X1DOT=X2
RETURN
END

```

```

FUNCTION X2DOT(T,X1,X2,A)
X2DOT=(1.0-A)/X1*X2*X2-T*X1*(1.0-A)*X2
RETURN
END

```

```

C**MULTIPLE CURVE PRINTER PLOT ROUTINE
C
C CALL: CALL W4PLOT(X,Y,N,NDIM,NCUR,ISCALE,XMIN,XMAX,YMIN,YMAX)
C
C PARAMETERS: X(I)=ARRAY OF X AXIS COORDINATES DIMENSIONED NDIM IN
C              THE CALLING PROGRAM.
C
C              Y(I,J)=ARRAY OF NCUR Y AXIS VARIABLES EACH OF LENGTH N.
C              THE FIRST VARIABLE IS STORED IN Y(I,1), THE
C              SECOND VARIABLE IN Y(I,2), ETC. DIMENSION OF Y IS
C              Y(NDIM,NCUR) IN THE CALLING PROGRAM.
C
C              N=NUMBER OF POINTS TO BE PLOTTED FOR EACH GRAPH.
C
C              ISCALE=SCALE CONTROL VARIABLE. IF ISCALE=0 THE PLOTS WILL
C              BE AUTOSCALED ON THE INPUT VARIABLES. IF ISCALE=1
C              THE SCALE IS SET IN X BY XMIN AND XMAX AND IN Y BY
C              YMIN AND YMAX.
C
C STORAGE: 639 DECIMAL WORDS
C
C DIMENSION XS(11),YS(17),X(1),Y(NDIM,NCUR)
C INTEGER#2IGRID(101),ICHAR(6)/1H+,1H*,1H$,1H=,1H.,1H /
C IF(ISCALE.EQ.1)GO TO 32
C XMAX=-1.0E+20
C XMIN=-XMAX
C YMAX=XMAX
C YMIN=-XMAX
C DO 25 I=1,N
C   IF(X(I).GT.XMAX)XMAX=X(I)
C   IF(X(I).LT.XMIN)XMIN=X(I)
C CONTINUE
C DO 31 J=1,NCUR
C DO 31 I=1,N
C   IF(Y(I,J).GT.YMAX)YMAX=Y(I,J)
C   IF(Y(I,J).LT.YMIN)YMIN=Y(I,J)
C CONTINUE
C 25 CONTINUE
C 31 CONTINUE
C 32 XR=XMAX-XMIN
C   IF(XR.EQ.0.0)XR=1.0E-20
C   YR=YMAX-YMIN
C   IF(YR.EQ.0.0)YR=1.0E-20
C   XT=XMAX*XMIN
C   YT=YMIN*YMAX
C   IF(XT.LT.0.0)IYAX=100.0*(-XMIN)/XR+1.5
C   IF(YT.LT.0.0)IXAX=64.0*YMAX/YR+1.5
C   XINCF=XR/10.0
C   YINCF=YR/16.0

```

```

XS(1)=XMIN
YS(1)=YMAX
DO 46 I=2,11
46 XS(I)=XS(I-1)+XINCR
DO 47 I=2,17
47 YS(I)=YS(I-1)-YINCR
WRITE(6,10)(XS(I),I=1,11)
II=1
KK=0
DO 146 IINF=1,65
DO 101 J=1,101
101 IGRID(J)=ICHAR(6)
IF(YT-GE.0.0)GO TO 109
IF(LINE-IXAX)109,104,109
104 DO 105 J=1,101
105 IGRID(J)=ICHAR(5)
106 IF(XT-LT.0.0)IGRID(IYAX)=ICHAR(5)
DO 125 J=1,NCUR
DO 125 I=1,N
IPTX=64.0*(YMAX-Y(I,J))/VXR+1.5
IF(IPTY-GT.65)IPTX=65
IF(IPTY-LT.1)IPTX=1
IF(IPTY-LINE)125,117,125
117 IPTX=100.0*(X(I)-XMIN)/XRR+1.5
JC=MDD(J,4)
IF(JC)119,118,119
118 IGRID(IPTX)=ICHAR(4)
GO TO 125
119 IGRID(IPTX)=ICHAR(JC)
125 CONTINUE
133 IF(KK)133,133,134
WRITE(6,20)YS(II),(IGRID(I),I=1,101),YS(II)
II=II+1
GO TO 135
134 WRITE(6,30)(IGRID(I),I=1,101)
135 KK=KK+1
IF(KK-4)146,136,146
136 KK=0
146 CONTINUE
WRITE(6,40)(XS(I),I=1,11)
RETURN
10 FORMAT(1H1,1PE15.2,10E10.2/10X,14*,20(5H+*****),2H+*)
20 FORMAT(1PE10.2,1H+,101A1,1H+,E9.2)
30 FORMAT(10X,1H*,101A1,1H*)
40 FORMAT(10X,1H*,20(5H+*****),2H+*/1PE16.2,10F10.2)
END

```

A P P E N D I X I I I

DIMENSIONLESS PLOT OF EXPERIMENTAL DATA AND BEST CURVE FIT

```
//PEN61227 JOB (1227,01FT) , 'FEDERICO A. PENARANDA', MSGLEVEL=1, CLASS=G
//EXEC FORTCLG, REGION.GC=160K, TIME.GC=10
```

PROGRAM PURPOSE.

FOR SHOCK TUBE INVESTIGATION OF THERMAL CONDUCTIVITY IN ARGON. THE PROGRAM IS WRITTEN TO SOLVE FOR THE VALUES OF QW (REFERENCE EQ.18) AND THE RATIO OF TEMPERATURES (REFERENCE EQ.15) HAVING AS INPUTS. P1, T0, TIME RESOLUTION AND VOLTAGE RISE IN HEAT TRANSFER THIN FILM GAUGE.

THE OUTPUT FOR THE FIRST PART IS A TABULAR SOLUTION PRINTING THE RESULTS AS WELL AS THE INITIAL DATA.

AFTER THE PARAMETERS QW AND THETA INFINITE HAS BEEN COMPUTED, THE SUBROUTINE DRAW IS CALLED, TO OBTAIN A GRAPHICAL REPRESENTATION OF THE EXPERIMENTAL RESULTS.

THEN SOLVING EQUATION 14, USING SUBROUTINE SYS2DE FOR DIFFERENT VALUES OF THE EXPONENT 'A', A PLOT OF THESE CURVES IS OBTAINED IN THE SAME GRAPH OF THE EXPERIMENTAL DATA, GIVEN THE BEST CURVE FIT FOR THE DIMENSIONLESS PLOT OF THETA INFINITE VS. QW.

```
REAL*8 LAB1/8H
DIMENSION X(54), Y(54,1), ERRSQ(47,50), SORET(50,1), XA(50),
*T(50), X1(50), X2(50), YY(47), LB(9), XC(24), YC(24)
READ(5,58) (ITITLE(I), I=1,12)
58 FORMAT(6A8)
59 READ(5,59) (LB(I), I=1,9)
59 FORMAT(9A4)
EXTERNAL X1DOT, X2DOT
N=0
WRITE(6,103)
103 FORMAT(1H1, T2, 'RUN', T14, 'P1', T27, 'T0', T38, 'DT', T48, 'DE', T59, 'MS',
*T67, 'DTEMP', T80, 'T5', T93, 'P5', T104, 'TW', T113, 'DINF', T126, 'QW', //)
*///)
```

```

cc READ(5,101) NR,PI, TQ, DT, DE
101 FORMAT(I2,8X,F20.0,3F10.0)
DE = DE#1.25
SMS = 151.765/(32100.*DT)
OTEMP = DE/.0016069
P5 = PI*((15.*SMS**4-8.*SMS**2 +1.)/(2.*SMS**2 +6.))
T5 = TQ*((13.*SMS**4 +2.*SMS**2 -1.)/(4.*SMS**2))
TW = DTEMP+TQ
OINF = T5/TW
DELP1 = 4.27+(0.0093*P5/760.)
DELP2 = 4.62+(0.0093*P5/760.)
DELPM = (DELP1+DELP2)/2.
AKW = DELPM+0.0138*(TW-310.5)
QW = 1704.16970*DTEMP/(AKW*P5*TW)**0.5
N = N+1
X(N) = QW
Y(N,1) = OINF
WRITE(6,102) NR,PI, TQ, DT, DE, SMS, DTEMP, T5, P5, TW, OINF, QW
102 IF(NR.LT.57) GO TO 99
L = 0
DO 590 NI = 1,47,2
L = L+1
XC(L) = X(NI)
YC(L) = Y(NI,1)
590 CONTINUE
CALL DRAW(24,XC,YC,1,3,LAB1,ITITLE,0.,0.,1,1,0,0,6,9,1,1,1,1,5,/)
TI=0.0
XII=1.0
H=C.01
K=10
DO 600 I=1,9
A=C.1 + (I-1)*0.1
DO 601 J = 1,47
X2I = X(J)
CALL SYS2DE(X1DCT,X2DCT,50,TI,XII,X2I,T,X1,X2,H,K,A)
YY(J) = X1(50)
601 CONTINUE
LAB = LB(I)
IF(I.LT.9) MCDCUR=2
IF(I.EQ.9) MCDCUR=3
CALL DRAW(47,X,YY,MCDCUR,0,LAB,ITITLE,0.,0.,1,1,0,0,6,9,1,1,1,1,5,/)
600 CONTINUE
STOP
END

```



```

SUBROUTINE SYS2DE (F,G,N,XI,YI,ZI,X,Y,Z,H,K,A)
DIMENSION X(1), Y(1), Z(1)
X(1)=XI
Y(1)=YI
Z(1)=ZI
DO 14 I=2,N
  U=X(I-1)
  V=Y(I-1)
  W=Z(I-1)
  DO 12 J=1,K
    S1=H*F(U,V,W,A)
    T1=H*G(U,V,W,A)
    S2=H*F(U+0.5*H, V+0.5*S1, W+0.5*T1,A)
    T2=H*G(U+0.5*H, V+0.5*S1, W+0.5*T1,A)
    S3=H*F(U+0.5*H, V+0.5*S2, W+0.5*T2,A)
    T3=H*G(U+0.5*H, V+0.5*S2, W+0.5*T2,A)
    S4=H*F(U+H, V+S3, W+T3,A)
    T4=H*G(U+H, V+S3, W+T3,A)
    U=U+H
    V=V+(S1+2.0*(S2+S3) + S4)/6.0
    W=W+(T1+2.0*(T2+T3) + T4)/6.0
  X(I)=U
  Y(I)=V
  Z(I)=W
  12 CONTINUE
  14 RETURN
END

FUNCTION X1DOT(T,X1,X2)
X1DOT=X2
RETURN
END

FUNCTION X2DOT(T,X1,X2,A)
X2DOT=(1.0-A)/X1*X2*X2-T*X1**(1.0-A)*X2
RETURN
END

```

INITIAL DISTRIBUTION LIST

	No. Copies
1. Defense Documentation Center Cameron Station Alexandria, Virginia 22314	20
2. Library Naval Postgraduate School Monterey, California 93940	2
3. Commander, Naval Air Systems Command Navy Department Washington, D. C. 20360	1
4. Commandante en Jefe de la Armada Correo Naval Santiago, Chile	1
5. Director Escuela Naval Arturo Prat Correo Naval Valparaiso, Chile	1
6. Director Escuela de Ingenieria Naval Correo Naval Valparaiso, Chile	1
7. Professor D. J. Collins Department of Aeronautics Naval Postgraduate School Monterey, California 93940	5
8. Chairman, Department of Aeronautics Naval Postgraduate School Monterey, California 93940	1
9. LCDR Federico A. Penaranda Base Aeronaval El Belloto Correo Naval Valparaiso, Chile	5

DOCUMENT CONTROL DATA - R & D

(Security classification of title, body of abstract and indexing annotation must be entered when the overall report is classified)

1. ORIGINATING ACTIVITY (Corporate author) Naval Postgraduate School Monterey, California 93940		2a. REPORT SECURITY CLASSIFICATION UNCLASSIFIED	
		2b. GROUP	
3. REPORT TITLE Shock Tube Investigation of Thermal Conductivity in Noble Gases			
4. DESCRIPTIVE NOTES (Type of report and, inclusive dates) Master's Thesis			
5. AUTHOR(S) (First name, middle initial, last name) Penaranda, Federico A., Lieutenant Commander, Chilean Navy			
6. REPORT DATE April, 1969		7a. TOTAL NO. OF PAGES 62	7b. NO. OF REFS 10
8a. CONTRACT OR GRANT NO.		9a. ORIGINATOR'S REPORT NUMBER(S)	
b. PROJECT NO.			
c.		9b. OTHER REPORT NO(S) (Any other numbers that may be assigned this report)	
d.			
10. DISTRIBUTION STATEMENT Distribution of this document is unlimited. This document has been approved for public release and sale; its distribution is unlimited.			
11. SUPPLEMENTARY NOTES		12. SPONSORING MILITARY ACTIVITY Naval Postgraduate School Monterey, California 93940	
13. ABSTRACT The Aeronautics Department shock tube has been developed and instrumented. The shock tube has been used in an experiment in which the thermal conductivity of argon has been determined in the temperature range of 1500 - 5000 °K and at relatively high pressures, 10 to 30 atmospheres.			

KEY WORDS

LINK A

LINK B

LINK C

ROLE

WT

ROLE

WT

ROLE

WT

shock tube

thermal conductivity

noble gases



thesP329

Shock tube investigation of thermal cond



3 2768 001 97948 7
DUDLEY KNOX LIBRARY